This is to certify that the
dissertation entitled

CHARACTERIZATION OF *Bacillus subtilis* UREASE AND
THE *Klebsiella aerogenes* UreEF PROTEIN

presented by

Jong Kyong Kim

has been accepted towards fulfillment
of the requirements for the

Ph.D. degree in Cell and Molecular Biology

Robert P. Hausinger
Major Professor's Signature

11/7/06
Date

MSU is an Affirmative Action/Equal Opportunity Institution

CHARACTERIZATION OF *Bacillus subtilis* UREASE AND THE *Klebsiella aerogenes* UreEF PROTEIN

By

Jong Kyong Kim

A DISSERTATION

Submitted to
Michigan State University
in partial fulfillment of the requirements
for the degree of

DOCTOR OF PHILOSOPHY

Cell and Molecular Biology Program

2006

ABSTRACT

CHARACTERIZATION OF *Bacillus subtilis* UREASE AND THE *Klebsiella aerogenes* UreEF PROTEIN

By

Jong Kyong Kim

In vivo assembly of the urease metallocenter in most bacteria typically requires the actions of four accessory proteins: UreD, UreE, UreF, and UreG. The urease gene cluster of *Bacillus subtilis* possesses only the structural genes (*ureABC*), and this organism lacks known accessory genes in its genome. Nevertheless, the organism can produce functional Ni-containing urease. The activation properties of recombinant *B. subtilis* urease were examined in both *Escherichia coli* and *B. subtilis* hosts. Overexpression of *B. subtilis ureABC* alone unexpectedly confers urease activity, however the level is low even in the presence of excess Ni in the cultures. Although the *B. subtilis* urease shares high sequence similarity to those of many other bacteria, it does not interact with other heterologous accessory proteins to enhance the urease activity. It still remains unclear whether the organism has unidentified non-homologous accessory gene(s) or if it lacks accessory genes in its genome so that its urease activates spontaneously.

The UreF accessory protein is poorly characterized because it is insoluble when *ureF* is overexpressed in *E. coli*. To produce a soluble form of UreF for biochemical and structural studies, the *K. aerogenes* UreEF fusion protein was generated by a translational fusion of *ureE* and *ureF*. The fusion protein was purified and biochemically characterized for oligomerization and metal binding

properties. The UreF portion of the UreEF is fully functional on the basis of its interactions with other urease components and its ability to activate urease. In contrast, the function of the UreE portion in UreEF was greatly compromised because the fusion prevented its dimerization and altered its metal binding properties as opposed to the wild type UreE. Serial deletion mutant studies on the UreEF protein provided the first evidence for the existence of distinct sub-domains of UreF. Finally, I propose a model for UreF action in urease activation by combining the results from my studies and previous investigations in the lab.

To my family,
with respect and love.

ACKNOWLEDGEMENTS

I would like to thank Dr. Robert Hausinger for being my advisor and providing me with great guidance and so much encouragement. I would also like to thank my committee members: Dr. Walter Esselman, Dr. Robert Britton, Dr. Michael Feig, and Dr. Shelagh Ferguson-Miller for their help and advice on my research. Especially, I would like to thank Dr. Britton for helping me with the *Bacillus subtilis* work. I greatly appreciate all of technical help and support from my lab members: Dr. Scott Mulrooney, Soledad Quiroz, Tina Müller, Piotr Grzyska, Jana Simmons, Efthalia Kalliri, Meng Li, Kimberly Anderson, Bruce Fraser, and Andrea Silva.

I would like to thank Dr. Sue Conrad for her understanding and support throughout my graduate study. Special thanks go out to Dr. Deug Y. Shin and Dr. Moo Je Cho for motivating me and giving me excellent training before I started my Ph.D. study.

Finally, I would like to thank my parents and brother for all the support and encouragement that they gave me during the years.

TABLE OF CONTENTS

LIST OF TABLES

LIST OF FIGURES

CHAPTER 1

INTRODUCTION

Part of this introduction is a modification of my contribution to a book chapter (Quiroz, S., J. K. Kim., S. B. Mulrooney, and R. P. Hausinger, "Chaperones of Nickel Metabolism" in volume 2 of the series *Metal Ions in Life Sciences*) that will be published in 2007.

Nickel is an essential micronutrient of many organisms where it serves as a cofactor for enzymes involved in several critical metabolic processes (1, 2). In contrast to its positive roles, the transition metal ion is toxic to cells; thus, synthesis of these Ni-enzymes requires the presence of carefully controlled Ni-processing mechanisms that range from selective transport of Ni into the cells to productive insertion of Ni into the apoproteins. Various accessory proteins participate in these processes and are required for the biosynthesis of several Ni-dependent enzymes. In this chapter, I provide brief overviews of the catalytic activities, biological roles, and active site architectures of eight crystallographically characterized Ni-dependent enzymes to illustrate the roles of nickel in various metabolic processes in microorganisms. I then focus this introduction on bacterial ureases, providing more detailed information on structural properties of urease, the process of urease activation, and biochemical/structural characteristics of urease accessory proteins. Finally, I present an outline of the remainder of my thesis by emphasizing the questions I sought to answer.

Ni-Containing Enzymes

Urease

Urease catalyzes the hydrolysis of urea to produce ammonia and carbamate. The latter molecule spontaneously decomposes to yield another molecule of ammonia and carbonic acid (Eqs. 1 and 2). This enzyme, found in plants, fungi and bacteria, has several biological roles (3). It participates in

recycling of environmental nitrogen by decomposing various sources of urea (including purines, amino acids, and urea fertilizers) to produce ammonia as a nitrogen source. In other cases, the enzyme functions as a virulence factor that is associated with gastric ulceration by *Helicobactor pylori* and urinary stone formation by *Proteus mirabilis*.

$$H_2N\text{-}CO\text{-}NH_2 + H_2O \rightarrow H_2N\text{-}COOH + NH_3 \qquad [1]$$

$$H_2N\text{-}COOH + H_2O \rightarrow H_2CO_3 + NH_3 \qquad [2]$$

Crystallographic analyses have revealed that most bacterial ureases possess three structural subunits (encoded by *ureA*, *ureB*, and *ureC*) associated into a trimer of trimers $[(\alpha\beta\gamma)_3]$, with each UreC subunit containing a dinuclear Ni active site bridged by a carbamylated Lys residue (4-6) (Figure 1A).

The urease gene cluster of most bacteria is composed of both structural genes (*ureABC*) and accessory genes (typically including *ureDEFG*, with additional urease-related genes present in some species). The structural gene products assemble into an apoprotein that requires activation by the accessory proteins. The best-studied urease activation system is that found in *Klebsiella aerogenes*, which contains the *ureDABCEFG* gene cluster (7, 8). Using this system, UreD, UreF, and UreG were identified as forming a GTP-dependent molecular chaperone that binds urease apoprotein (9), while UreE was shown to function as a metallochaperone that delivers Ni (10, 11). The detailed structural properties of urease and its activation process will be presented later in this chapter.

Figure 1. Active sites of structurally-characterized Ni-containing enzymes. In each case, Ni is shown as a solid black sphere except for CODH (C), other metals are shown in gray, and the remaining features are depicted in outline. A. Dinuclear Ni-Ni active site of urease (PDB code 1FWJ). The metal-bridging side chain is a carbamylated Lys. B. Dinuclear Ni-Fe active site of a [NiFe] hydrogenase (PDB code 1CC1). The Ni is bound to three Cys and one seleno-Cys (or in other cases to four Cys), two of which also coordinate the Fe. The Fe-bound diatomic ligands are two cyanide and one carbon monoxide molecules. C. [Ni-Fe_4-S_5] cluster of CODH (PDB code 1SU8). The structure of this site slightly varies in other CODH sites. D. [4Fe-4S]-Ni-Ni site of ACS (PDB code 1OAO). The central Ni is coordinated by three Cys and an unknown ligand depicted in gray eclipse. E. F_{430} Ni-tetrapyrrole of methyl coenzyme M reductase (PDB code 1MRO). F. The active site of Ni-SOD (PDB code 1T6U). G. Ni-glyoxylase showing two bound water molecules (PDB code 1F9Z). H. Ni-containing form of aci-reductone dioxygenase as derived by a combination of solution structure analysis and homology modeling (PDB code 1M4O).

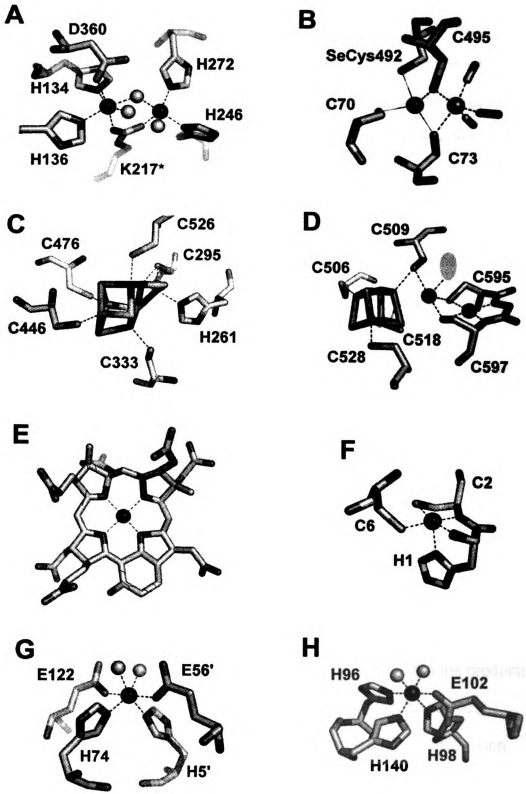
A
D360
H272
H134
H246
H136
K217*
B
C495
SeCys492
C70
C73
C
C526
C476
C295
C446
H261
C333
D
C509
C506
C595
C518
C528
C597
E
F
C2
C6
H1
G
E122
E56'
H74
H5'
H
H96
E102
H140
H98

Hydrogenase

Hydrogenases catalyze the reversible oxidation of molecular hydrogen into protons and electrons (Eq. 3). These enzymes provide a mechanism for many microorganisms to use H_2 as an energy source by generating a proton gradient or to remove excess reducing power in the form of molecular hydrogen (12).

$$H_2 \leftrightarrow 2\ H^+ + 2\ e^- \qquad [3]$$

Three distinct classes of hydrogenases are defined by the metal content of their active sites: [NiFe]-hydrogenases, [Fe]-hydrogenases, and [iron-sulfur-cluster-free]-hydrogenases (12, 13). The crystal structures of several [NiFe]-hydrogenases have been resolved, including those of *Desulfovibrio gigas* and *Desulfomicrobium baculatum* (14-16). Each heterodimeric protein has three iron-sulfur clusters in their small subunit and a [NiFe] active site in their large subunit. The active center contains Ni coordinated by four Cys residues (or three Cys and a selenocysteine in the *D. baculatum* enzyme), two of which bridge to the Fe that is also liganded by one carbon monoxide and two cyanide groups (Figure 1B).

Seven accessory proteins are required to synthesize the *Escherichia coli* HycGE NiFe-hydrogenase (17), the paradigm system for defining the activation process of these enzymes (18, 19). These accessory proteins are the products of the six *hyp* genes (*hypABCDEF*) and another gene encoding a specific endopeptidase (*hycI*). The current model of HycE (large subunit) maturation includes a complicated series of steps involving [1] HypDEF-mediated formation of an $Fe(CN)_2(CO)$ site in a process facilitated by HypC (20); [2] insertion of Fe

and its ligands into the precursor of the large subunit (retaining its C-terminal extension) when in complex with HypC (21); [3] GTP-dependent addition of Ni to the active center mediated by HypAB; and [4] proteolytic processing of the C-terminus of HycE by HybD, leading to internalization of the catalytic center. Carbamoylphosphate (CP) was shown to be the precursor of the CN ligands (22), but CO is generated using a distinct substrate (23). HypF displays CP phosphatase activity and catalyzes a CP-dependent pyrophosphate ATP exchange reaction (24). More importantly, HypF catalyzes the ATP-dependent transfer of the carbamoyl group of CP to the C-terminal Cys of HypE (25). The ATP-dependent dehydration of the thiocarbamoyl moiety by HypE results in thiocyanated HypE which can provide the CN ligand to Fe (25). HypC is a central protein in the metallocenter assembly process (20, 21), and is presumed to serve as a molecular chaperone. HypA and HypB together appear to function as the Ni metallochaperone, with the latter protein also suggested to have a molecular chaperone role. The HycI endopeptidase subsequently cleaves off the C-terminal extension of HycE after Ni insertion, and the truncated protein binds to the small subunit and becomes membrane associated. HybD, a homolog of HycI that is specific to hydrogenase 2, has been structurally characterized and shown to possess a pentacoordinate Cd atom at the active site (26). The apoprotein form of the endopeptidase is proposed to bind to hydrogenase-bound Ni (coordinated by only three Cys ligands), thus activating the protease to cleave the correct peptide bond in the hydrogenase subunit (27-29).

Carbon Monoxide Dehydrogenase (CODH)

CODHs catalyze the reversible oxidation of carbon monoxide to carbon dioxide (Eq. 4). Organisms possessing these enzymes play critical roles in the global carbon cycle and the degradation of environmental pollutants (30).

$$CO + H_2O \leftrightarrow CO_2 + 2H^+ + 2e^- \quad [4]$$

Crystal structures are known for CODHs from *Carboxydothermus hydrogenoformans* and *Rhodospirillum rubrum* (31, 32). Both proteins are ~ 130-kDa homodimers containing five metal-sulfur clusters of three types (B, C, and D) in a C-B'-D-B-C' arrangement where the D cluster bridges the two subunits. While the B, B' and D sites are the same cubane type [4Fe-4S] clusters in both proteins, the structures of the active site clusters (C and C') slightly differ in the two proteins. The C cluster of *R. rubrum* is essentially a [1Ni-3Fe-4S] cubane bridged to a mononuclear Fe site, whereas the structure of the *C. hydrogenoformans* enzyme can be viewed as a [3Fe-4S] cluster fused with a [Ni-S-Fe] fragment containing a bridging sulfide (Figure 1C).

Information regarding the mechanism of Ni insertion into CODH is available for *R. rubrum* where the *cooCTJ* gene cluster (33), located downstream of the *cooS* structural gene, is known to be involved. The CooC protein, which contains a nucleotide-binding motif, acts as an ATP/GTP-dependent molecular chaperone, while CooJ delivers Ni by using its histidine-rich C-terminal motif.

Acetyl-CoA Synthase/CODH (ACS/CODH)

The CODH activity described above is found in another set of enzymes isolated from acetogenic bacteria and methanogenic archaea. The ACS/CODHs are bifunctional catalysts that exhibit the activity shown in Eq. 4 and additionally

synthesize (or decompose) acetyl-coenzyme A (CoA-SH) using the remarkable chemistry shown in Eq. 5. The CODH site of ACS/CODH reduces CO_2 to CO and then this gaseous molecule traverses a molecular tunnel within the protein to reach the ACS site where it is joined to CoA-SH and the methyl group from the corrinoid-iron-sulfur protein (Co-FeSP). Along with the monofunctional CODHs, these enzymes play a major role in the global carbon cycle and in the formation and removal of greenhouse gases (34).

$$CO + CoA\text{-}SH + CH_3\text{-}Co(III)\text{-}FeSP \leftrightarrow CH_3C(O)\text{-}S\text{-}CoA + Co(I)\text{-}FeSP \quad [5]$$

Crystallographic studies of *Moorella thermoacetica* ACS/CODH revealed that the tetrameric protein contains the dimeric CODH subunits at its core and one ACS subunit on each end (35, 36). The ACS metallocenter is a [4Fe-4S]-Ni-Ni site called the A-cluster. The [4Fe-4S] cluster is bridged to one Ni via a Cys side chain, and this metal is in turn bridged by two Cys residues to a second Ni, that is additionally bound by two backbone amides (Figure 1D). The central Ni in the A-cluster is subject to metal substitution, resulting in inactive Cu-Ni and Zn-Ni species that were critical to identifying closed and open conformations of the protein. The [4Fe-4S]-Ni-Ni cluster also was observed in the structure of the monomeric *C. hydrogenoformans* ACS (37).

Little is known about the mechanism concerning metallocenter assembly in ACS/CODHs. Since the enzyme has two different sets of Ni-containing active sites, it is anticipated that several accessory proteins are required for biosynthesis. Consistent with this notion, ACS/CODH gene clusters contain

several non-subunit open reading frames (ORFs). In particular, AcsF encodes a CooC-like protein.

Methyl Coenzyme M Reductase

Methyl coenzyme M reductase catalyzes the reaction of methyl-*S*-coenzyme M (CH_3-S-CoM, where CoM-SH is 2-thioethanesulfonate) with coenzyme B (CoB-SH, *N*-7-mercaptoheptanoylthreonine phosphate) to form methane and the heterodisulfide, CoM-S-S-CoB (Eq. 6). This is the final step of methane formation in methanogenic archaea growing on simple molecules such as acetate, methanol, formate, and carbon dioxide plus hydrogen gas (38).

$$CH_3\text{-S-CoM} + \text{CoB-SH} \rightarrow CH_4 + \text{CoB-S-S-CoM} \qquad [6]$$

The X-ray crystal structure of methyl coenzyme M reductase, first obtained from *Methanothermobacter marburgensis* (39), reveal that the protein is a 300-kDa heterohexamer of three different subunits ($\alpha_2\beta_2\gamma_2$) containing two molecules of the Ni-containing tetrapyrrole, F_{430} (Figure 1E). This cofactor, named on the basis of its characteristic absorbance maximum at 430 nm when in the Ni(II) state, must be in the Ni(I) state for the enzyme to be active. Each active site F_{430} is buried deep in the protein and accessible from the surface by a 50 Å long channel composed of mainly hydrophobic amino acids through which CH_3-S-CoM can enter, and which is blocked by the binding of CoB-SH.

The biosynthetic pathway of F_{430} is an offshoot of those for other biological tetrapyrroles (40). Early labeling studies demonstrated that F_{430} is derived from dihydrosirohydrochlorin, which is also the precursor of siroheme and corrinoids. The dihydrosirohydrochlorin is formed from 5-aminolevulinic acid via

uroporphyrinogen III. The conversion of dihydrosirohydrochlorin to F_{430} requires several steps including amidation of acetate groups on two rings, reduction of two double bonds, cyclization of an acetamide to form the five-membered ring, cyclization of a propionic acid to form the six-membered ring, and insertion of Ni. However, the order of these steps and the mechanism underlying the Ni insertion and F_{430} incorporation into the protein remain unknown.

Superoxide Dismutase (SOD)

SODs are ubiquitous metalloenzymes that function to protect biological molecules from oxidative damage by catalyzing the dismutation of superoxide anion radicals to peroxide and molecular oxygen (Eq. 7). In addition to the well-known Cu,Zn-, Fe-, and Mn-containing SODs, recent studies have revealed the existence of Ni-SODs in *Streptomyces* species and some cyanobacteria.

$$2\ O_2^- + 2\ H^+ \rightarrow H_2O_2 + O_2 \qquad [7]$$

Crystal structures of Ni-SODs have been solved for *S. seoulensis* and *S. coelicolor* enzymes (41, 42). The proteins are homohexamers consisting of four-helix bundle subunits. The N-terminal loop coordinates the active site Ni(III) in square pyramidal geometry using two thiolate side chains (Cys-2 and Cys-6), two backbone amides (His-1 and Cys-2), and the His-1 side chain ligand at the axial position (Figure 1F). The axial ligand is lost in the reduced state, with Ni(II) becoming square planar. Apoprotein structures show that the residues involved in binding Ni are disordered.

Ni-SODs in *Streptomyces* species are products of *sodN*, which encodes a preprotein with an N-terminal extension of 14 amino acids. During SOD

maturation, proteolytic cleavage precedes Ni binding and results in the creation of the six-residue Ni-binding site. Recently, ORFs with significant homology to Ni-SODs were identified in the genomes of several cyanobacteria including *Prochlorococcus marinus* MIT9313 (43). In this microbe, an ORF located downstream of *sodN* and named *sodX* was suggested to be the peptidase for maturation of the Ni-SOD. Coexpression of *sodX* and *sodN* in an oxygen-sensitive *E. coli* strain restored oxygen tolerance in a Ni-dependent manner, indicating the production of a catalytically active enzyme and providing confirmatory evidence for the importance of SodX in Ni-SOD maturation. Ni-SOD activity in *S. seoulensis* is stimulated by the overproduction of CbiXhp, a Ni-binding protein, suggesting that it may function in metallocenter assembly (44). Contrary to this notion, the gene encoding CbiXhp is located between two genes suggested to function in cobalamin biosynthesis. Further studies are needed to elucidate the detailed maturation steps of Ni-SOD activation, including the mechanism of Ni incorporation to the enzyme.

Glyoxylase

Glyoxylase I (Glx I) is the first of two enzymes in the pathway to convert cytotoxic methylglyoxal into non-toxic α-hydroxycarboxylic acids. It converts the hemimercaptal substrate, formed nonenzymatically from methylglyoxal and glutathione (GSH, Eq. 8), to non-toxic *S*-D-lactoylglutathione (Eq. 9), which is the substrate for Glx II (Eq. 10). These enzymes are important for cellular protection because methylglyoxal can exert toxic effects by reacting with DNA, RNA and proteins.

CH_3-CO-CHO + GSH ↔ CH_3-CO-C(OH)-SG [8]

CH_3-CO-C(OH)-SG → CH_3-CH(OH)-CO-SG [9]

CH_3-CH(OH)-CO-SG + H_2O → CH_3-CH(OH)-COOH + GSH [10]

Unlike the case for Glx I of humans, *Saccharomyces cerevisiae*, and *Pseudomonas putida*, where the active site metal is zinc, Glx I from *E. coli* is completely inactive in the presence of Zn and is maximally active with Ni (45). Reduced activity is found in the enzyme substituted with Co, Cd, and Mn. Crystallographic analyses revealed that catalytically active forms of *E. coli* Glx I with Ni, Co, and Cd each have octahedral metal coordination (Figure 1G), which is also observed in the Zn-containing human enzyme, whereas the inactive Zn-containing *E. coli* protein displays a five-coordinate metal site (46). Several other pathogenic microorganisms are hypothesized to possess a Ni-containing glyoxylase on the basis of sequence comparisons (47). The cellular mechanism of Ni incorporation into Glx I is unknown.

Aci-Reductone Dioxygenase (ARD)

Many microorganisms utilize the methionine salvage pathway to regenerate methionine from methylthioadenosine, produced during polyamine biosynthesis from *S*-adenosylmethionine. Aci-reductone is a key intermediate of this pathway, and is oxidized to two different sets of products in *Klebsiella pneumoniae*. One oxidation pathway leads to production of formate and the ketoacid precursor of methionine. The other route of oxidation, a non-productive pathway, converts the aci-reductone to formate, carbon monoxide, and methylthiobutyric acid. Remarkably, the two reactions are carried out by the

same enzyme, ARD, depending on which metal is bound at the active site (Fe or Ni, respectively) (48).

The solution structure of *K. pneumoniae* Ni-ARD was determined by NMR methods (49). The enzyme is a monomer containing two β-sheets that hinge together to form a jellyroll. Unfortunately, paramagnetism of the bound Ni causes broadening of the ^{1}H resonance lines from residues near the metal center, thus hindering the structural characterization of the active site. Biophysical studies suggest the presence of three His ligands to the Ni, along with three other nitrogen or oxygen atoms (50). Homology modeling of the active center, based on the structure of jack bean canavalin (another member of the cupin family), provides a reasonable model of the active site (Figure 1H). The mechanism of Ni insertion into the enzyme is unknown.

Structural properties of urease. The structures of bacterial ureases and their dinuclear nickel active sites have been resolved by crystallographic methods using enzymes from *K. aerogenes* (4, 5), *Bacillus pasteurii* (6), and *H. pylori* (51). These studies reveal that most bacterial ureases possess three structural subunits associated into a trimer of trimers $[(\alpha\beta\gamma)_3]$ with UreA ~ 11 kDa, UreB ~ 12-14 kDa, and UreC ~ 60 kDa. Each UreC subunit contains a dinuclear nickel active site buried in an $(\alpha\beta)_8$-barrel structure with an active site flap composed of two major helices. The active site is coordinated by four histidines, one aspartate, one carbamylated lysine (bridging the two nickel ions separated by 3.6 Å), one bridging water, and two terminal water molecules (Figure 1A). The

nickel to which the oxygen of urea is expected to bind is pentacoordinate in distorted square-pyramidal geometry with the carbamylated lysine at the apex, while the other nickel is hexacoordinate in distorted octahedral geometry with the carbamylated lysine and aspartate as opposing apical ligands (3).

In contrast to this common theme, the *H. pylori* enzyme has only two subunits, a ~ 26.5 kDa UreA (corresponding to a fusion of the two small subunits in other bacteria) and a ~ 61.7 kDa UreB large subunit, forming a $(\alpha_3\beta_3)_4$ supramolecular structure (51). Plants and fungi have a single subunit corresponding to a fusion of all of the bacterial subunits, assembled into an α_6 urease structure that resembles a dimer of the bacterial urease (52). Despite these differences in quaternary structure, all urease sequences are highly conserved and the metallocenters are believed to be identical (1).

Accessory genes for urease activation in bacteria. Urease gene clusters in most bacteria contain structural genes encoding the urease subunits and accessory genes required for biosynthesis of catalytically active enzyme (by assisting in proper assembly of the metallocenter). Although genetic organization of the urease gene cluster may vary in different organisms, four accessory genes (*ureD*, *ureE*, *ureF*, and *ureG*) are typically found in the common three-subunit urease systems. For example, the *K. aerogenes* urease operon has *ureD* gene located upstream of the *ureABC* structural genes followed by *ureE*, *ureF*, and *ureG* (7, 8). In case of *Bacillus pasteurii* (53) and *Yersinia enterocolitica* (54), all four accessory genes are placed downstream of the structural genes in a

ureEFGD arrangement. In some species, additional urease-related genes are present in their urease clusters. For example, the *ureI* of *H. pylori* (55) or *ureH* of *Bacillus* sp. TB-90 (56) plays specialized functions (such as a urea channel) that are not required for the synthesis of active urease.

Recent advances in microbial genome projects have made more than 200 complete genome sequences available, and approximately 20 % of these contain homologues to *ureC* gene. As described above, most bacteria have the structural genes clustered with the accessory genes in various arrangements. In selected microorganisms, however, the urease genes are interrupted by long intervening sequences or some (or all) of the common accessory genes are absent from the urease operon. The detailed examples will be discussed in Chapter 2. Among these atypical urease systems, *Bacillus subtilis ure* operon has the most striking feature; i.e., it contains homologues to *ureABC*, but has no counterparts to *ureDEFG* in its genome. Nevertheless, this organism was shown to produce active enzyme and utilize urea as sole nitrogen source (57). A series of studies (Chapters 2 and 3) were carried out to better understand the urease activation process in this microorganism.

Urease activation. Assembly of the urease metallocenter is a complicated process involving nickel, carbon dioxide (used for carbamylation of the bridging lysine residue), several accessory proteins, and GTP hydrolysis (1). In our earlier studies on the *K. aerogenes* urease, various multi-protein complexes, composed of apoenzyme and accessory proteins, were purified and

examined for their activation properties (9, 11, 58-60). UreD-, UreDF-, UreDFG-urease apoprotein complexes have been studied and shown to possess distinct activation properties when compared to those of the urease apoprotein alone. Briefly, about 15 % of the apoprotein is activated *in vitro* by addition of Ni and bicarbonate (for carbamylation of the active site Lys residue), whereas about 30 % of the urease within the UreD-urease apoprotein is activated by these conditions, demonstrating that UreD directly facilitates this process (58). Furthermore, the UreDF-urease apoprotein is activated to the same extent by using almost 1000-fold lower concentrations of bicarbonate, and the activation of this complex is resistant to inactivation by high concentrations of Ni (59). A UreDFG-urease apoprotein complex forms upon addition of UreG to the UreDF-urease apoprotein, and exhibits GTP-dependent urease activation which is not achieved with a nucleotide-binding motif (P-loop) defective UreG mutant or a non-hydrolyzable GTP analog (9). Finally, when the UreE metallochaperone is added to this complex along with GTP and near-physiological levels of Ni and bicarbonate, fully active enzyme is generated (11). These *in vitro* activation and other related studies on urease apoprotein complexes provided valuable insight into how the urease metallocenter is synthesized *in vivo*, and began to identify the distinct roles for some of the accessory proteins at different steps of the assembly process. According to the current urease activation model, urease apoprotein sequentially binds the accessory proteins—first generating the UreD-urease apoprotein complex, followed by binding of UreF, and finally UreG (60). UreD, UreF, and UreG in combination are proposed to form a GTP-dependent

molecular chaperone ensuring productive conformations of the apoproteins for proper metal incorporation (9), while UreE functions as a metallochaperone that binds and delivers Ni to the apoprotein complex (10, 11). Upon activation, all accessory proteins dissociate from the complex, as evidenced by structures of holoenzyme. It is not yet clear, however, how the GTP hydrolysis is coupled to the Ni insertion event. Therefore, it is imperative to elucidate detailed functions of each accessory protein at a biochemical and structural level and to establish protein-protein interactions among the urease components in this multi-protein complex. In the next section, biochemical and structural findings on these urease accessory proteins and their interactions will be summarized.

Biochemical and structural properties of urease accessory proteins

Urease metallochaperone. Among the various accessory proteins required for urease activation, UreE functions as a metallochaperone that delivers Ni to the urease apoprotein. Sequence analysis of UreE in several microorganisms reveal that the carboxyl termini of these proteins contain His-rich regions indicative of a potential metal binding function. For example, *K. aerogenes* UreE has 10 His in the last 15 residues, and the C-terminal His-rich region of *P. mirabilis* UreE contains 9 His in the last 10 residues (7, 61). Metal binding studies showed that the *K. aerogenes* UreE binds about 6 Ni per dimer (62), while *B. pasteurii* UreE (containing only two His residues in this region) binds a single Ni per dimeric protein (63). Purified UreE proteins also bind other metal ions such as Cu and Zn, suggesting that the specificity of urease for Ni is

not determined solely by this delivery protein (64). Site-directed mutagenesis was used to create a truncated form of *K. aerogenes* UreE lacking the last 15 residues (His144*UreE), and studies with the shortened UreE revealed that the His-rich region is not essential for urease activation; i.e., the truncated UreE can still bind 2-3 Ni per dimer and activate urease *in vivo* in a Ni-dependent manner (65). Further site-directed mutagenesis and structural studies provided detailed information on metal binding properties of UreE. Variants of *K. aerogenes* His144*UreE affecting His110 or His112 exhibit reduced Ni binding while not greatly inhibiting urease activation, whereas a variant affecting His96 binds less Ni and abolishes its ability to activate urease (66). Crystallographic analyses of Cu-bound *K. aerogenes* His144*UreE revealed that the critical His96 residue is located at the dimer interface coordinating a metal by using a pair of His96 on each subunit (67). Similar results were observed from the crystal structures of *B. pasteurii* UreE where a pair of His100 residues coordinates a Zn at the dimer interface (68). The overall structures of both proteins are nearly identical, but the *K. aerogenes* protein has two additional metal binding sites involving His110 and His112, one at each subunit. Another difference between the two structures is that the crystallization conditions (i.e., high protein concentrations) promote oligomerization of the *B. pasteurii* protein to form a dimer of dimers where all four His100 side chains work as a ligand to a single Zn.

Several studies indicated that UreE interacts with other urease accessory proteins during metallocenter assembly. *In vitro* activation studies with the *K. aerogenes* urease showed that UreDFG-urease apoprotein complex is fully

activated only in the presence of UreE with Ni, bicarbonate, and GTP (11), strongly suggesting that UreE functions as a metallochaperone to deliver Ni to the apoprotein complex, and that substantial protein-protein interactions may exist between UreE and other urease components within the apoprotein complex. Consistent with this hypothesis, a yeast two-hybrid study demonstrated that UreE interacts with UreG in *H. pylori* (69).

Although UreE is believed to play the role of metallochaperone in most cases, the situation appears to be more complicated in *H. pylori*. Deletion of either *hypA* or *hypB* gene (normally associated with hydrogenase maturation) was shown to negatively affect urease activity which could be restored by addition of excess Ni (70). This result suggests that the HypA and HypB proteins are involved in urease activation as metallochaperones in addition to the UreE present in this microorganism.

Urease molecular chaperone components. UreD, UreF, and UreG are thought to form a GTP-dependent molecular chaperone during urease activation (9). Among these accessory proteins, only UreG is highly soluble enabling biochemical and structural characterization of the protein. The *K. aerogenes* UreG is a monomer that is unable to bind or hydrolyze GTP by itself although this protein has a nucleotide-binding (P-loop) motif associated with GTP-dependent urease activation (71). In contrast, UreG from *B. pasteurii*, which is more than 50 % identical to the *K. aerogenes* counterpart, is dimeric and has weak GTPase activity (72). The purified *B. pasteurii* protein was also shown to bind 2 Zn per

dimer with a K_d of 42 μM or 4 Ni per dimer with weak affinity (K_d 360 μM). The NMR structure of *B. pasteurii* UreG suggests that the protein is intrinsically disordered. Unlike UreG, very little is known about UreD and UreF as individual proteins because they are insoluble when overexpressed in *E. coli*. As an attempt to obtain a soluble form of UreF for biochemical and structural characterization, *K. aerogenes* UreEF fusion protein was created by a translational fusion of *ureE* to *ureF*, which will be described in Chapter 4.

Although there is only limited information on the urease molecular chaperone components as individual proteins, several studies were carried out to investigate the protein-protein interactions among the urease components either as individual proteins or within various apoprotein complexes composed of UreABC subunits and the molecular chaperone components. A yeast two-hybrid analysis of the *H. pylori* system indicated that UreF interacts with UreH (corresponding to UreD in other microorganisms), but not with UreG (69). A similar approach using the *P. mirabilis* urease components also revealed that UreF interacts with UreD, with additional homomultimeric interactions of UreD and UreF (73). Subsequent chemical cross-linking/tryptic digestion/mass spectrometry studies suggested that UreF interacts with UreD-urease apoprotein complex to induce a conformational change within urease that may enhance access of Ni to the active site buried in the enzyme (74).

Thesis outline

The following chapters describe my studies on characterization of *Bacillus subtilis* urease and the *Klebsiella aerogenes* UreEF fusion protein. In Chapter 2, I provide evidence that *B. subtilis* can produce active Ni-dependent urease and utilize urea as sole nitrogen source, despite the lack of known urease accessory genes in its genome. Recombinant *B. subtilis* urease was produced in both *E. coli* and *B. subtilis* hosts and examined for its activation properties. Finally, complementation studies with other heterologous accessory genes were performed. The studies described in Chapter 2 were published in J. Bacteriol. **187:** 7150-4 (2005). In Chapter 3, I describe a further study regarding the *B. subtilis* urease to determine whether the organism has unidentified non-homologous accessory gene(s) or if it lacks accessory genes in its genome so that its urease activates spontaneously. In particular, I created a *B. subtilis* genomic library and used it to screen for novel non-homologous accessory gene(s) or potential urease enhancing factors. In Chapter 4, I describe the generation of a *K. aerogenes* UreEF fusion protein by a translational fusion of the *ureE* and *ureF* genes in an effort to produce a soluble form of the UreF protein. The fusion protein was purified and biochemically characterized for oligomerization and metal binding properties. I also describe protein-protein interactions involving this fusion protein and their correlation to urease activation. The studies described in this chapter will be published in J. Bacteriol. Finally, Chapter 5 contains a related study on the UreEF fusion protein examining the

interactions between the UreEF and UreG. Based on the studies I conducted above, I present a refined version of urease activation model and discuss the remaining questions regarding the urease metallocenter assembly and possible future research directions to answer part of these questions.

References

1. Mulrooney, S. B. and Hausinger, R. P. Nickel uptake and utilization by microorganisms. FEMS Microbiol. Rev., 27: 239-261, 2003.

2. Hausinger, R. P. Biochemistry of Nickel, p. 280. New York: Plenum Publishing, 1993.

3. Hausinger, R. P. and Karplus, P. A. Urease. In: K. Wieghardt, R. Huber, T. L. Poulos, and A. Messerschmidt (eds.), Handbook of Metalloproteins, pp. 867-879. West Sussex, U.K.: John Wiley & Sons, Ltd., 2001.

4. Jabri, E., Carr, M. B., Hausinger, R. P., and Karplus, P. A. The crystal structure of urease from *Klebsiella aerogenes*. Science, 268: 998-1004, 1995.

5. Pearson, M. A., Michel, L. O., Hausinger, R. P., and Karplus, P. A. Structure of Cys319 variants and acetohydroxamate-inhibited *Klebsiella aerogenes* urease. Biochemistry, 36: 8164-8172, 1997.

6. Benini, S., Rypniewski, W. R., Wilson, K. S., Miletti, S., Ciurli, S., and Mangani, S. A new proposal for urease mechanism based on the crystal structures of the native and inhibited enzyme from *Bacillus pasteurii*: why urea hydrolysis costs two nickels. Structure, 7: 205-216, 1999.

7. Mulrooney, S. B. and Hausinger, R. P. Sequence of the *Klebsiella aerogenes* urease genes and evidence for accessory proteins facilitating nickel incorporation. J. Bacteriol., 172: 5837-5843, 1990.

8. Lee, M. H., Mulrooney, S. B., Renner, M. J., Markowicz, Y., and Hausinger, R. P. *Klebsiella aerogenes* urease gene cluster: sequence of ureD and demonstration that four accessory genes (*ureD*, *ureE*, *ureF*, and *ureG*) are involved in nickel metallocenter biosynthesis. J. Bacteriol., 174: 4324-4330, 1992.

9. Soriano, A. and Hausinger, R. P. GTP-dependent activation of urease apoprotein in complex with the UreD, UreF, and UreG accessory proteins. Proc. Natl. Acad. Sci. USA, 96: 11140-11144, 1999.

10. Colpas, G. J. and Hausinger, R. P. In vivo and in vitro kinetics of metal transfer by the *Klebsiella aerogenes* urease nickel metallochaperone, UreE. J. Biol. Chem., 275: 10731-10737, 2000.

11. Soriano, A., Colpas, G. J., and Hausinger, R. P. UreE stimulation of GTP-dependent urease activation in the UreD-UreF-UreG-urease apoprotein complex. Biochemistry, 39: 12435-12440, 2000.

12. Vignais, P. M. and Colbeau, A. Molecular biology of microbial hydrogenases. Curr. Issues Molec. Biol., 6: 159-188, 2004.

13. Vignais, P. M., Billoud, B., and Meyer, J. Classification and phylogeny of hydrogenases. FEMS Microbiol. Rev., 25: 455-501, 2001.

14. Volbeda, A., Charon, M.-H., Piras, C., Hatchikian, E. C., Frey, M., and Fontecilla-Camps, J. C. Crystal structure of the nickel-iron hydrogenase from *Desulfovibrio gigas*. Nature (London), 373: 580-587, 1995.

15. Garcin, E., Vernede, X., Hatchikian, E. C., Volbeda, A., Frey, M., and Fontecilla-Camps, J. C. The crystal structure of a reduced [NiFeSe] hydrogenase provides an image of the activated catalytic center. Structure, 7: 557-566, 1999.

16. Volbeda, A., Garcin, E., Piras, C., de Lacey, A. L., Fernandez, V. M., Hatchikian, E. C., Frey, M., and Fontecilla-Camps, J. C. Structure of the [NiFe] hydrogenase active site: evidence for biologically uncommon Fe ligands. J. Am. Chem. Soc., 118: 12989-12996, 1996.

17. Lutz, A., Jacobi, A., Schlensog, V., Böhm, R., Sawers, G., and Böck, A. Molecular characterization of an operon (hyp) necessary for the activity of the three hydrogenase isoenzymes in *Escherichia coli*. Molec. Microbiol., 5: 123-135, 1991.

18. Blokesch, M., Paschos, A., Theodoratou, E., Bauer, A., Hube, M., Huth, S., and Böck, A. Metal insertion into NiFe-hydrogenases. Biochem. Soc. Trans., 30: 674-680, 2002.

19. Casalot, L. and Rousset, M. Maturation of [NiFe] hydrogenases. Trends Microbiol., 9: 228-237, 2001.

20. Blokesch, M., Albracht, S. P. J., Matzanke, B. F., Drapal, N., Jacobi, A., and Böck, A. The complex between hydrogenase-maturation proteins HypC and HypD is an intermediate in the supply of cyanide to the active site iron of [NiFe]-hydrogenases. J. Molec. Biol., 344: 155-167, 2004.

21. Blokesch, M. and Böck, A. Maturation of [NiFe]-hydrogenases in *Escherichia coli*: the HypC cycle. J. Molec. Biol., 324: 287-296, 2002.

22. Paschos, A., Glass, R. S., and Böck, A. Carbamoylphosphate requirement for synthesis of the active center of [NiFe]-hydrogenases. FEBS Lett., 488: 9-12, 2001.

23. Roseboom, W., Blokesch, M., Böck, A., and Albracht, S. P. J. The biosynthetic routes for carbon monoxide and cyanide in the Ni-Fe active site of hydrogenases are different. FEBS Lett., 579: 469-472, 2005.

24. Paschos, A., Bauer, A., Zimmermann, A., Zehelein, E., and Böck, A. HypF, a carbamoyl phosphate converting enzyme involved in [NiFe]-hydrogenase maturation. J. Biol. Chem., 277: 49945-49951, 2002.

25. Reissmann, S., Hochleitner, E., Wang, H., Paschos, A., Lottspeich, F., Glass, R. S., and Böck, A. Taming of a poison: biosynthesis of the NiFe-hydrogenase cyanide ligands. Science, 299: 1067-1070, 2003.

26. Fritsche, E., Paschos, A., Beisel, H.-G., Böck, A., and Huber, R. Crystal structure of the hydrogenase maturating endopeptidase HYBD from *Escherichia coli*. J. Molec. Biol., 288: 989-998, 1999.

27. Theodoratou, E., Paschos, A., Magalon, A., Fritsche, E., Huber, R., and Böck, A. Nickel serves as a substrate recognition motif for the endopeptidase involved in hydrogenase maturation. Eur. J. Biochem., 267: 1995-1999, 2000.

28. Theodoratou, E., Paschos, A., Mintz-Weber, S., and Böck, A. Analysis of the cleavage site specificity of the endopeptidase involved in the maturation of the large subunit of hydrogenase 3 from *Escherichia coli*. Arch. Microbiol., 173: 110-116, 2000.

29. Theodoratou, E. and Böck, A. [NiFe]-hydrogenase maturation endopeptidase: structure and function. Biochem. Soc. Trans., 33: 108-111, 2005.

30. Lindahl, P. A. The Ni-containing carbon monoxide dehydrogenase family: light at the end of the tunnel? Biochemistry, 41: 2097-2105, 2002.

31. Dobbek, H., Svetlitchnyi, V., Gremer, L., Huber, R., and Meyer, O. Crystal structure of a carbon monoxide dehydrogenase reveals a [Ni-4Fe-5S] cluster. Science, 293: 1281-1285, 2001.

32. Drennan, C. L., Heo, J., Sintchak, M. D., Schreiter, E., and Ludden, P. W. Life on carbon monoxide: X-ray structure of *Rhodospirillum rubrum* Ni-Fe-S carbon monoxide dehydrogenase. Proc. Natl. Acad. Sci. USA, 98: 11973-11978, 2001.

33. Kerby, R. L., Ludden, P. W., and Roberts, G. P. In vivo nickel insertion into carbon monoxide dehydrogenase of *Rhodosprillum rubrum*: molecular and physiological characterization of cooCTJ. J. Bacteriol., 179: 2259-2266, 1997.

34. Drennan, C. L., Doukov, T. I., and Ragsdale, S. W. The metalloclusters of carbon monoxide dehydrogenase/acetyl-CoA synthase: a story in pictures. J. Biol. Inorg. Chem., 9: 511-515, 2004.

35. Doukov, T. I., Iverson, T. M., Seravalli, J., Ragsdale, S. W., and Drennan, C. L. A Ni-Fe-Cu center in a bifunctional carbon monoxide dehydrogenase/acetyl-CoA synthase. Science, 298: 567-272, 2002.

36. Darnault, C., Volbeda, A., Kim, E. J., Legrand, P., Vernede, X., Lindahl, P. A., and Fontecilla-Camps, J. C. Ni-Zn-[Fe_4S_4] and Ni-Ni-[Fe_4S_4] clusters in closed and open subunits of acetyl-CoA synthase/carbon monoxide dehydrogenase. Nature Structure Biology, 10: 271-279, 2003.

37. Svetlitchnyi, V., Dobbek, H., Meyer-Klaucke, W., Meins, T., Thiele, B., Römer, P., Huber, R., and Meyer, O. A functional Ni-Ni-[4Fe-4S] cluster in the monomeric acetyl-CoA synthase from *Carboxydothermus hydrogenoformans*. Proc. Natl. Acad. Sci. USA, 101: 446-451, 2004.

38. Thauer, R. K. Biochemistry of methanogenesis: a tribute to Marjory Stephenson. Microbiol., 144: 2377-2406, 1998.

39. Ermler, U., Grabarse, W., Shima, S., Goubeaud, M., and Thauer, R. K. Crystal structure of methyl-coenzyme M reductase: the key enzyme of biological methane formation. Science, 278: 1457-1462, 1997.

40. Thauer, R. K. and Bonacker, L. G. Biosynthesis of coenzyme F430, a nickel porphinoid involved in methanogenesis. Ciba Foundation Symposium, 180: 210-227, 1994.

41. Wuerges, J., Lee, J.-W., Yim, Y.-I., Kang, S. O., and Carugo, K. D. Crystal structure of nickel-containing superoxide dismutase reveals another type of active site. Proc. Natl. Acad. Sci. USA, 101: 8569-8574, 2004.

42. Barondeau, D. P., Kassman, C. J., Bruns, C. K., Tainer, J. A., and Getzoff, E. D. Nickel superoxide dismutase structure and mechanism. Biochemistry, 43: 8038-8047, 2004.

43. Eitinger, T. In vivo production of active nickel superoxide dismutase from *Prochlorococcus marinus* MIT9313 is dependent on its cognate peptidase. J. Bacteriol., 186: 7812-7825, 2004.

44. Kim, I.-K., Yim, Y.-I., Kim, Y.-M., Lee, J.-W., Yim, H.-S., and Kang, S.-O. CbiX-homologous protein (CbiXhp), a metal-binding protein, from *Streptomyces seoulensis* is involved in expression of nickel-containing superoxide dismutase. FEMS Microbiol. Lett., 228: 21-26, 2003.

45. Clugston, S. L., Barnard, J. F. J., Kinach, R., Miedema, D., Ruman, R., Daub, E., and Honek, J. F. Overproduction and characterization of a dimeric non-zinc glyoxylase I from *Escherichia coli*: evidence for optimal activation by nickel ions. Biochemistry, 37: 8754-8763, 1998.

46. He, M. M., Clugston, S. L., Honek, J. F., and Matthews, B. W. Determination of the structure of *Escherichia coli* glyoxylase I suggests a structural basis for differential metal activation. Biochemistry, 39: 8719-8727, 2000.

47. Clugston, S. L. and Honek, J. F. Identification of sequences encoding the detoxification metalloisomerase glyoxylase I in microbial genomes from several pathogenic organisms. J. Molec. Evol., 50: 491-495, 2000.

48. Dai, Y., Wensink, P. C., and Abeles, R. H. One protein, two enzymes. J. Biol. Chem., 274: 1193-1195, 1999.

49. Pochapsky, T. C., Pochapsky, S. S., Ju, T., Mo, H., Al-Mjeni, F., and Maroney, M. J. Modeling and experiment yields the structure of acireductone dioxygenase from *Klebsiella pneumoniae*. Nature Structure Biology, 9: 966-972, 2002.

50. Al-Mjeni, F., Ju, T., Pochapsky, T. C., and Maroney, M. J. XAS investigation of the structure and function of Ni in acireductone dioxygenase. Biochemistry, 41: 6761-6769, 2002.

51. Ha, N.-C., Oh, S.-T., Sung, J. Y., Cha, K.-A., Lee, M. H., and Oh, B.-H. Supramolecular assembly and acid resistance of *Helicobacter pylori* urease. Nature Structure Biology, 8: 505-509, 2001.

52. Sheridan, L., Wilmont, C. M., Cromie, K. D., van der Logt, P., and Phillips, S. E. V. Crystallization and preliminary X-ray structure determination of jack bean urease with a bound antibody fragment. Acta Crystallogr., D58: 374-376, 2001.

53. Kim, S. D. and Hausinger, R. P. Genetic organization of the recombinant *Bacillus pasteurii* urease genes expressed in *Escherichia coli*. J. Microbiol. Biotechnol., 4: 108-112, 1994.

54. de Koning-Ward, T. F., Ward, A. C., and Robins-Browne, R. M. Characterization of the urease-encoding gene complex of *Yersinia enterocolitica*. Gene, 145: 25-32, 1994.

55. Weeks, D. L., Eskandar, S., Scott, D. R., and Sachs, G. A H^+-gated urea channel: the link between *Helicobacter pylori* urease and gastric colonization. Science, 287: 482-485, 2000.

56. Maeda, M., Hidaka, M., Nakamura, A., Masaki, H., and Uozumi, T. Cloning, sequencing, and expression of thermophilic *Bacillus* strain TB-90 urease gene complex in *Escherichia coli*. J. Bacteriol., 176: 432-442, 1994.

57. Cruz-Ramos, H., Glaser, P., Wray, L. V., Jr., and Fisher, S. H. The *Bacillus subtilis* ureABC operon. J. Bacteriol., 179: 3371-3373, 1997.

58. Park, I.-S., Carr, M. B., and Hausinger, R. P. In vitro activation of urease apoprotein and role of UreD as a chaperone required for nickel metallocenter assembly. Proc. Natl. Acad. Sci. USA, 91: 3233-3237, 1994.

59. Moncrief, M. B. C. and Hausinger, R. P. Purification and activation properties of UreD-UreF-urease apoprotein complexes. J. Bacteriol., 178: 5417-5421, 1996.

60. Park, I.-S. and Hausinger, R. P. Evidence for the presence of urease apoprotein complexes containing UreD, UreF, and UreG in cells that are competent for in vivo enzyme activation. J. Bacteriol., 177: 1947-1951, 1995.

61. Jones, B. D. and Mobley, H. L. T. *Proteus mirabilis* urease: nucleotide sequence determination and comparison with jack bean urease. J. Bacteriol., 171: 6414-6422, 1989.

62. Lee, M. H., Pankratz, H. S., Wang, S., Scott, R. A., Finnegan, M. G., Johnson, M. K., Ippolito, J. A., Christianson, D. W., and Hausinger, R. P. Purification and characterization of *Klebsiella aerogenes* UreE protein: a nickel-binding protein that functions in urease metallocenter assembly. Prot. Sci., 2: 1042-1052, 1993.

63. Ciurli, S., Safarof, N., Miletti, S., Dikiy, A., Christensen, S. K., Kornetzky, K., Bryant, D. A., Vandenberghe, I., Devreese, B., Samyn, B., Remaut, H., and Van Beeumen, J. Molecular characterization of *Bacillus pasteurii* UreE, a metal-binding chaperone for the assembly of the urease active site. J. Biol. Inorg. Chem., 7: 623-631, 2002.

64. Colpas, G. J., Brayman, T. G., McCracken, J., Pressler, M. A., Babcock, G. T., Ming, L.-J., Colangelo, C. M., Scott, R. A., and Hausinger, R. P. Spectroscopic characterization of metal binding by *Klebsiella aerogenes* UreE urease accessory protein. J. Biol. Inorg. Chem., 3: 150-160, 1998.

65. Brayman, T. G. and Hausinger, R. P. Purification, characterization, and functional analysis of a truncated *Klebsiella aerogenes* UreE urease accessory protein lacking the histidine-rich carboxyl terminus. J. Bacteriol., 178: 5410-5416, 1996.

66. Colpas, G. J., Brayman, T. G., Ming, L.-J., and Hausinger, R. P. Identification of metal-binding residues in the *Klebsiella aerogenes* urease nickel metallochaperone, UreE. Biochemistry, 38: 4078-4088, 1999.

67. Song, H. K., Mulrooney, S. B., Huber, R., and Hausinger, R. P. Crystal structure of *Klebsiella aerogenes* UreE, a nickel-binding metallochaperone for urease activation. J. Biol. Chem., 276: 49359-49364, 2001.

68. Remaut, H., Safarov, N., Ciurli, S., and Van Beeumen, J. Structural basis for Ni(2+) transport and assembly of the urease active site by the metallochaperone UreE from *Bacillus pasteurii*. J. Biol. Chem., 276: 49365-49370, 2001.

69. Rain, J.-C., Selig, L., de Reuse, H., Battaglia, V., Reverdy, C., Simon, S., Lenzen, G., Petel, F., Wojcik, J., Schächter, V., Chemama, Y., Labigne, A., and Legrain, P. The protein-protein interaction map of *Helicobacter pylori*. Nature, 409: 211-215, 2001.

70. Olson, J. W., Mehta, N. S., and Maier, R. J. Requirement of nickel metabolism proteins HypA and HypB for full activity of both hydrogenase and urease in *Helicobacter pylori*. Molec. Microbiol., 39: 176-182, 2001.

71. Moncrief, M. B. C. and Hausinger, R. P. Characterization of UreG, identification of a UreD-UreF-UreG complex, and evidence suggesting that a nucleotide-binding site in UreG is required for in vivo metallocenter assembly of *Klebsiella aerogenes* urease. J. Bacteriol., 179: 4081-4086, 1997.

72. Zambelli, B., Stola, M., Musiani, F., De Vriendt, K., Samyn, B., Devreese, B., Van Beeumen, J., Dikiy, A., Bryant, D. A., and Ciurli, S. UreG, a chaperone in the urease assembly process, is an intrinsically unstructured GTPase that specifically binds Zn^{2+}. J. Biol. Chem., 280: 4684-4695, 2005.

73. Heimer, S. R. and Mobley, H. L. Interaction of *Proteus mirabilis* urease apoprotein and accessory proteins identified with yeast two-hybrid technology. J. Bacteriol., 183: 1423-1433, 2001.

74. Chang, Z., Kuchar, J., and Hausinger, R. P. Chemical crosslinking and mass spectrometric identification of sites of interaction for UreD, UreF, and urease. J. Biol. Chem., 279: 15305-15313, 2004.

CHAPTER 2

Characterization of *Bacillus subtilis* urease

These studies were published in *J. Bacteriol.* 187: 7150-4, 2005.

ABSTRACT

Most bacterial urease operons are composed of both structural genes (*ureA*, *ureB*, and *ureC*) that encode urease apoprotein and accessory genes (*ureD*, *ureE*, *ureF*, and *ureG*) that encode proteins required for the GTP-dependent incorporation of nickel. Genome sequence analysis has revealed that *Bacillus subtilis* contains only the urease structural genes. Despite the lack of known urease accessory genes, this organism exhibits urease activity and can grow using urea as sole nitrogen source. Here, I confirm that *B. subtilis* possesses a functional urease and demonstrate that the recombinant enzyme produced in *Escherichia coli* confers low levels of urease activity in a nickel-dependent manner. Unlike other well-characterized ureases, *B. subtilis* urease is sensitive to high salt concentrations that induce dissociation of UreA and precipitation of UreBC. Although *B. subtilis* urease shares high sequence similarity to the *Klebsiella aerogenes* and *Bacillus pasteurii* proteins, coexpression studies revealed no complementation of the *B. subtilis* urease genes by accessory genes from these microorganisms. While *B. subtilis* urease does not interact with established urease accessory proteins to enhance the incorporation of nickel into its active site, it remains possible that unidentified accessory proteins are utilized *in vivo* and evidence consistent with this possibility are summarized.

INTRODUCTION

Urease is a nickel-containing enzyme found in plants, fungi, and bacteria (17). This protein has several biological roles including its participation in recycling of environmental nitrogen and its capacity to serve as a virulence factor in pathogenic microorganisms that are associated with gastric ulceration and urinary stone formation (25).

Most bacterial ureases possess three structural subunits (encoded by *ureA*, *ureB*, and *ureC*) associated into a trimer of trimers [$(\alpha\beta\gamma)_3$], with each UreC subunit containing a dinuclear nickel active site bridged by a carbamylated lysine (4, 18, 32). Helicobacter species have only two subunits (UreA, corresponding to a fusion of the small subunits (β and γ) in other bacteria, and the large subunit, labeled UreB) in a $(\alpha_3\beta_3)_4$ macromolecular structure (16). Fungi and plants contain a single subunit, a fusion of the three bacterial sequences, in a homohexameric (α_6) structure (36).

The synthesis of active urease in most organisms requires the action of several accessory proteins (27). The best-studied urease activation system is that found in *Klebsiella aerogenes* where the structural genes are found in a gene cluster containing four accessory genes (*ureDABCEFG*). Using this system, UreD, UreF, and UreG were identified as forming a GTP-dependent molecular chaperone that binds urease apoprotein (9, 38), while UreE was shown to function as a metallochaperone by delivering nickel (13, 29, 37).

Genome sequence analysis has revealed that, in contrast to the situation found in other ureolytic microorganisms, *Bacillus subtilis* contains only the urease structural genes (*ureABC*) and lacks homologues to the accessory genes (20). Despite this dearth of urease genes, the organism exhibits urease activity and can grow using urea as sole nitrogen source (14).

Here, I confirm that *B. subtilis* synthesizes a functional urease, demonstrate that recombinant *B. subtilis* enzyme produced in *Escherichia coli* confers weak urease activity in a nickel-dependent manner, identify a unique salt-dependent lability of the *B. subtilis* enzyme resulting in dissociation of UreA with precipitation of UreBC, and show that accessory proteins from *K. aerogenes* or *B. pasteurii* are unable to enhance activation of *B. subtilis* urease. In addition, I review sequence evidence identifying other urealytic microorganisms that lack one or more urease accessory gene(s) and I highlight several dinuclear hydrolases, related to urease, that are activated without the participation of specific accessory proteins.

MATERIALS AND METHODS

Construction of clones. All molecular biology methods followed the standard protocol outlined in Sambrook et al. (35). Primers (Table 1) were synthesized at Integrated DNA Technologies, Inc. (Coralville, Iowa) for construction of plasmids used in this study (Table 2). Site-directed mutagenesis was performed to introduce an *Nde*I site into pURE91 (generously provided by

TABLE 1. Primers used in this study

Plasmid generated	Primers[a]
pURE93	For: GAAGGAGGACTACATATGAAACTGACACCAGTTG
	Rev: CAACTGGTGTCAGTTTCATATGTAGTCCTCCTTC
pKAU602	For: GGAATTACATATGGAACTGACCCCCCGAGAAAAA
	Rev: CGGAATTCTTAAAACAGAAAATATCGTTGCGCCATCGG
pACT-	For: TCCCCCGGGGCACAATTGGTTTGTGCAACGATTCAC
BpEFGD	Rev: ACGCGTCGACCCGATTGAAAGGAATAGTGAATGCGCA
pACT-	Left: CATAACGTTCTCTTAAGTCAGCCAGATTCG
ABCdel	Right: CCGATGGCGCAACGATATTTTCTGTTT
pDR-	For: CACGCGTCGACGCCGCTTTGAAAGGCATCTTACCGTAT
BsABC	Rev: CCTAGCTAGCTTAGTCAATAGAACGGCCGGATGCACT

[a] Locations of restriction sites are underlined

TABLE 2. Plasmids used

Plasmid	Characteristics	Reference
pURE91	*B. subtilis ureABC* genes cloned into pET-23	S. Fisher
pET-42b	Cloning and expression vector	Novagen
pURE93	*B. subtilis ureABC* genes cloned into pET-42b	This study
pKK17	*K. aerogenes ureDABCEFG* genes on an *Eco*RI-*Hin*dIII fragment cloned into pKK223-3	(12)
pKAU602	*K. aerogenes ureABC* genes cloned into pET-42b	This study
pACT3	Cloning and expression vector	(15)
pACT-KKWT	*K. aerogenes ureDABCEFG* genes cloned into pACT3	(29)
pACT-ABCdel	*K. aerogenes ureDEFG* genes in pACT3 formed by deleting *ureABC* genes from pACT-KKWT	This study
pBU11	*B. pasteurii ureABCEFGD* genes cloned into pBR322	(19)
pACT-BpEFGD	*B. pasteurii ureEFGD* genes cloned into pACT3	This study
pDR111	Cloning and expression vector for *Bacillus*	(8)
pDR-BsABC	*B. subtilis ureABC* genes cloned into pDR111	This study

Susan Fisher), a pET-23 derived plasmid containing *B. subtilis ureABC*, to allow for removal of the urease structural genes by double digestion with *Nde*I and *Xho*I. The resulting DNA fragment covering the entire *B. subtilis* urease operon was cloned into pET-42b to yield pURE93. pKAU602 (containing *K. aerogenes ureABC*) and pACT-BpEFGD (encoding *Bacillus pasteurii ureEFGD*) were generated by conventional PCR-based cloning procedures using pKK17 (33) and pBU11 (19) as templates and pET-42b and pACT3 as vectors, respectively. Each amplified DNA fragment was digested with the appropriate restriction enzymes, with the cleavage sites indicated in Table 1, and cloned into the indicated expression vector that had been digested with the corresponding enzymes. pACT-ABCdel was constructed by deleting the *ureABC* region from the intact *K. aerogenes* urease operon in pACT-KKWT (29) by using the QuickChange mutagenesis kit (Statagene). To construct pDR-BsABC, pURE91 was used as a template for amplifying the DNA fragment covering the *B. subtilis ureABC* genes that were subsequently digested with *Sal*I and *Nhe*I and cloned into pDR111 (8). All the plasmids were verified by sequencing throughout the entire open reading frames.

Bacterial strains and culture conditions. *E coli* C41(DE3) cells (23) were used as host for expression for all plasmids except for pDR-BsABC. *E. coli* transformants were cultured in Terrific Broth (TB, Fisher Biotech) supplemented with appropriate antibiotics and 7 mM $NiCl_2$ unless otherwise indicated. These cultures were grown at 37 °C to OD_{600} ~ 0.4, induced with 0.5 mM isopropyl β-D-thiogalactopyranoside (IPTG, Roche), and harvested after 14-16 hr. *B. subtilis*

SF10 (wild type, SMY derivative, from Dr. Susan Fisher) cells were cultured in S7 medium (43). *B. subtilis* RB247 (*trpC2 pheA1*, from Dr. Rob Britton) was transformed with pDR-BsABC as described (8) and grown in LB medium supplemented with 0.5 mM $NiCl_2$.

Preparation of cell extracts. Cell pellets were resuspended in 20 mM Tris-Cl buffer (pH 7.4) containing 150 mM NaCl and 1 mM EDTA (STE buffer), and disrupted by sonication (Branson Sonifier). Intact cells and debris were removed by centrifugation at 10,000 *g* for 20 min at 4 °C.

Polyacrylamide gel electrophoresis. Sodium dodecyl sulfate (SDS)-polyacrylamide gel electrophoresis (PAGE) was carried out for protein analysis with the buffers described by Laemmli (21) and utilized 15% polyacrylamide running gels with 4.5% stacking gels. The gels were stained with Coomassie brilliant blue (Sigma).

Urease and protein assays. Urease activity was measured by quantifying the rate of ammonia release from the hydrolysis of urea by formation of indophenol, which was monitored at 625 nm (44). One unit of urease activity (U) was defined as the amount of enzyme required to hydrolyze 1 μmol of urea per min at 37 °C. The standard assay buffer contained 50 mM *N*-2-hydroxyethylpiperazine-*N'*-ethanesulfonic acid (HEPES; pH 7.8) and 50 mM urea. Protein concentrations were determined by using a commercial assay (Bio-Rad) with bovine serum albumin as the standard (6).

In vitro activation. Standard activation conditions for the various urease apoprotein samples utilized the conditions established for activation of *K.*

aerogenes urease apoprotein (30, 31). Thus, the samples were added to 100 mM HEPES (pH 8.3), 150 mM NaCl, 100 mM $NaHCO_3$, and 300 μM $NiCl_2$ and incubated at 37 °C for 90 min. These conditions were modified for specific experiments by varying the nickel ion concentration, adding alternative metal ions, changing the pH, or altering the bicarbonate concentration.

Enrichment of *B. subtilis* urease. Cell extracts of *E. coli* C41(DE3) carrying plasmid pURE91 were prepared as described above, except that the STE buffer was replaced by 20 mM potassium phosphate, 1 mM EDTA, and 1 mM β-mercaptoethanol (PEB; pH 7.4) containing 0.5 mM phenylmethylsulfonyl fluoride for resuspension of the cells. The standard purification procedures established for the *K. aerogenes* urease (42), which employ chromatography on DEAE-Sepharose and phenyl Sepharose resins (Pharmacia) in PEB buffers with added KCl, resulted in the loss of *B. subtilis* urease activity. As an alternative enrichment procedure, the cell extracts containing *B. subtilis* urease were subjected to the more gentle purification conditions of gel filtration chromatography (Sephacryl S-300, Pharmacia) using STE buffer containing 150 mM NaCl. On the basis of the integrated intensities (Kodak 1D Scientific Imaging Systems) of urease bands after denaturing polyacrylamide gel analysis, the enriched *B. subtilis* urease was estimated to be > 85% homogeneous.

Metal analysis. Protein samples were subjected to repeated concentration / dilution cycles using a centricon-100 filter (Millipore) with metal-free water (inductively coupled plasma emission (ICP)-grade water) to remove buffer and excess metal ions. After determination of protein concentrations, the

samples were adjusted to contain 5 % nitric acid and centrifuged to obtain the protein-free solution for metal analysis. The Chemical Analysis Laboratory at University of Georgia determined the metal contents of urease preparations by ICP spectroscopy.

RESULTS

Urease activity in *B. subtilis*. To confirm that *B. subtilis* urease is biologically functional, SF10 cells were examined for their ability to grow in minimal medium using urea as the limiting nitrogen source. In a modification of the procedure described by Cruz-Ramos et al (14), SF10 cells were cultured in S7 medium plus glutamate, washed with S7 medium lacking any nitrogen source, and distributed into fresh S7 medium containing no nitrogen source, 0.2 % glutamate, or 0.2 % urea. As illustrated in Figure 1, the culture lacking a nitrogen source failed to grow whereas cultures provided with glutamate or urea exhibited similar rates of growth as indicated by the increased turbidity of the cultures. These results indicate that *B. subtilis* urease activity can support cell growth using urea as the sole nitrogen source.

Consistent with the observed growth on urea as nitrogen source, low but detectable urease activity was detected in cell extracts of *B. subtilis* SF10 cultured under nitrogen-limited growth conditions (0.113 ± 0.006 U/mg protein). This level of activity is comparable to the 0.103 ± 0.012 U/mg (after correction to

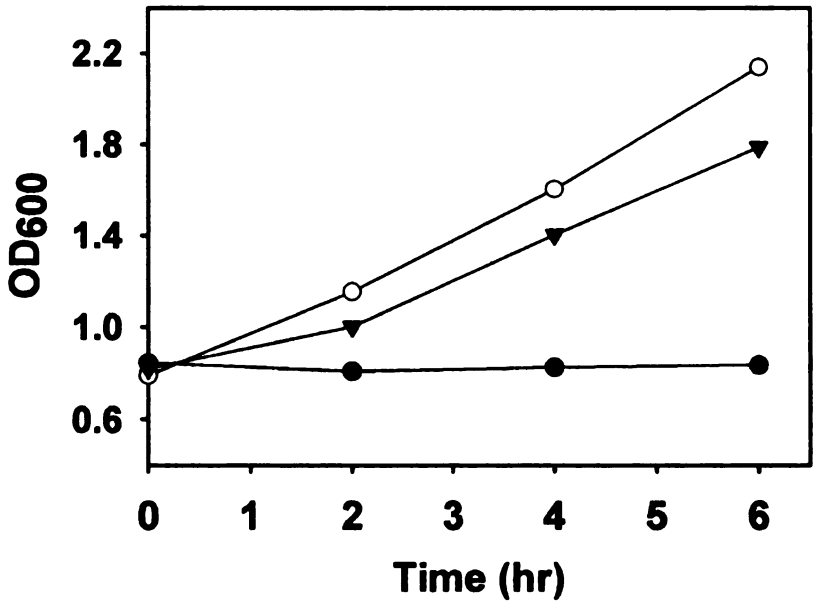

Figure 1. Growth of *B. subtilis* in S7 minimal medium containing varied nitrogen sources. Samples were removed at the indicated times for measurement of OD_{600}. Symbols: ●, no added nitrogen; ○, 0.2% glutamate; ▼, 0.2% urea.

the same units) described previously for extracts of these cells (3), and compares to the 2,500 U/mg for purified *K. aerogenes* urease (41). The addition of supplementary nickel ions to the culture (100 μM) had little to no effect on the urease activity (0.107 ± 0.016 U/mg protein), which suggests that either the trace levels of nickel ions in the S7 minimal medium were sufficient for synthesis of active urease or this enzyme might not require nickel for activation.

Purified urease apoprotein of *K. aerogenes* is known to undergo partial activation when incubated with nickel ions plus bicarbonate (used as a source of CO_2 for carbamylation of the active site lysine to form the requisite metal-bridging ligand) (18, 30, 31); thus, cell extracts of *B. subtilis* were examined to determine whether its urease could be activated using the same protocol. Rather than undergoing activation, the observed urease activity decreased by 50%.

Overexpression of *B. subtilis ureABC* in *B. subtilis*. The observation that supplementary nickel in the culture medium exerted no effects on the urease activity in cell extracts of *B. subtilis* SF10 led us to test the effects of urease overexpression in *B. subtilis* cells. I reasoned that trace levels of nickel ions in the medium may be sufficient for synthesis of active urease in wild-type *B. subtilis*, which expresses only very low levels of urease, whereas nickel-dependent activity might be observed in a strain that overproduces the urease protein. To test this possibility, pDR-BsABC encoding *B. subtilis* urease was introduced into RB247, a closely related wild-type *B. subtilis*, to overproduce the enzyme in *B. subtilis*. As shown in Figure 2, urease gene expression in the *B. subtilis* transformant was greatly enhanced by IPTG induction in LB medium

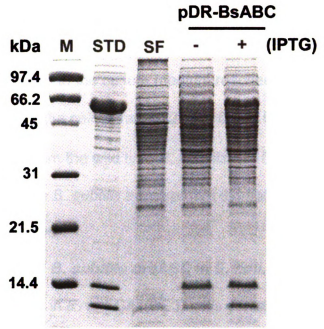

Figure 2. Expression of recombinant *B. subtilis ureABC* in *B. subtilis*. Cultures of *B. subtilis* RB247 cells transformed with pDR-BsABC were induced with 0.5 mM IPTG and the cell extracts were analyzed by denaturing polyacrylamide gel. Lanes: 1, molecular weight markers (phosphorylase b, M_r 97,400; bovine serum albumin, M_r 66,200; ovalbumin, M_r 45,000; carbonic anhydrase, M_r 31,000; soybean trypsin inhibitor, M_r 21,000; lysozyme, M_r 14,400); 2, enriched *B. subtilis* urease standard; 3, cell extracts of SF10 cells grown in S7 minimal medium with glutamate as nitrogen source; 4 and 5, cell extracts of *B. subtilis* transformant.

while SF10 cell extracts exhibited no visible urease proteins. Despite the larger amount of urease protein in the cell extracts of the *B. subtilis* transformant, the activity was lower (0.081 ± 0.026 U/mg) than in the wild-type strain. The addition of nickel ions (0.5 mM) to the culture medium resulted in ~ 3.5-fold increase in the urease activity of the cell extract (0.281 ± 0.105 U/mg), which is still comparable to that from the wild type *B. subtilis* SF10. In vitro activation using the cell extracts of the *B. subtilis* transfromant did not increase the activity any further (data not shown).

Expression of *B. subtilis ureABC* in *E. coli*. Recombinant *B. subtilis* urease was produced in *E. coli* C41(DE3) cells containing pURE91, which includes the entire coding region of *B. subtilis ureABC*. Urease gene expression was highly induced by the addition of IPTG to the TB medium (Figure 3); however, the urease activity measured in cell extracts was very low (0.14 ± 0.02 U/mg protein). Growth of the *E. coli* transformant in TB medium containing varied nickel concentrations revealed that urease activity was nickel-dependent, with maximal activity of 6.4 ± 0.9 U/mg protein observed when the medium was supplemented with 5-7 mM $NiCl_2$ (higher nickel concentrations led to cell toxicity) (Figure 4).

Activation properties of recombinant *B. subtilis* urease. For cells grown in TB medium containing 7 mM $NiCl_2$, only modest increases in urease activity (< 10 %) were observed when cell extracts were subjected to standard activation conditions. In contrast, significant urease activation was observed in cell extracts made from cells grown in TB medium lacking supplemental nickel as

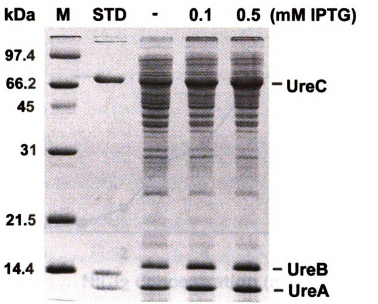

Figure 3. Expression of recombinant *B. subtilis* urease in *E. coli*. The effect of varied IPTG concentration on expression of recombinant *B. subtilis* urease genes in *E. coli* C41 (pURE91) cell extracts was monitored by denaturing polyacrylamide gel analysis. Lane 1, molecular weight markers; lane 2, 6 μg of purified *K. aerogenes* urease; lane 3, uninduced control; lanes 4 and 5, extracts of the cells induced with 0.1 mM and 0.5 mM IPTG, respectively.

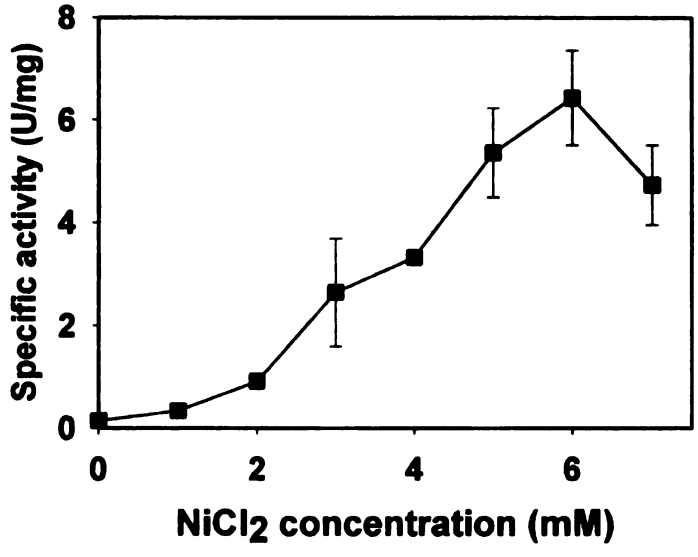

Figure 4. Effect of nickel concentration on recombinant *B. subtilis* urease activity. Cells were cultured in TB medium supplemented with the indicated nickel concentrations and urease activities were assayed in the cell extracts. Error bars represent the standard deviation for three separate determinations.

depicted in Figure 5. This figure also reveals the effects of varied concentrations of $NiCl_2$ and several other divalent cations on activation of the enzyme in the cell extracts. Among the divalent cations tested, nickel ions resulted in the largest enzyme activation while manganese ions activated the enzyme to a small extent and the other metal ions had negligible effects (Figure 5). Notably, manganese ions also have been shown to activate *K. aerogenes* urease apoprotein, yielding ~2 % of the activity generated by nickel ion activation (30, 45). The growth studies with varied nickel ion concentrations and the in vitro activation results both suggest that the *B. subtilis* urease is a nickel-containing enzyme, like all other ureases that have been characterized (17).

Characterization of recombinant *B. subtilis* urease. In order to understand why urease activity was so low in *E. coli* C41(DE3) cells containing pURE91, even when grown with high concentrations of nickel ion in the medium and despite the observed high-level production of the urease subunits, I attempted to characterize the properties of the isolated enzyme. Unfortunately, all efforts to purify the recombinant urease by using ion exchange and hydrophobic interaction chromatography resins, even in the presence of potential stabilizing agents such as glycerol and reductant, resulted in losses of activity. Although the basis of *B. subtilis* urease inactivation is not completely defined, high levels of salts (0.5-1.5 M KCl) led to UreA dissociating from the heterotrimeric enzyme, with UreBC precipitating out of solution. To overcome the apparent enzyme instability, the urease was enriched from cell extracts by use of gel filtration chromatography in the presence of 150 mM NaCl. Two independent

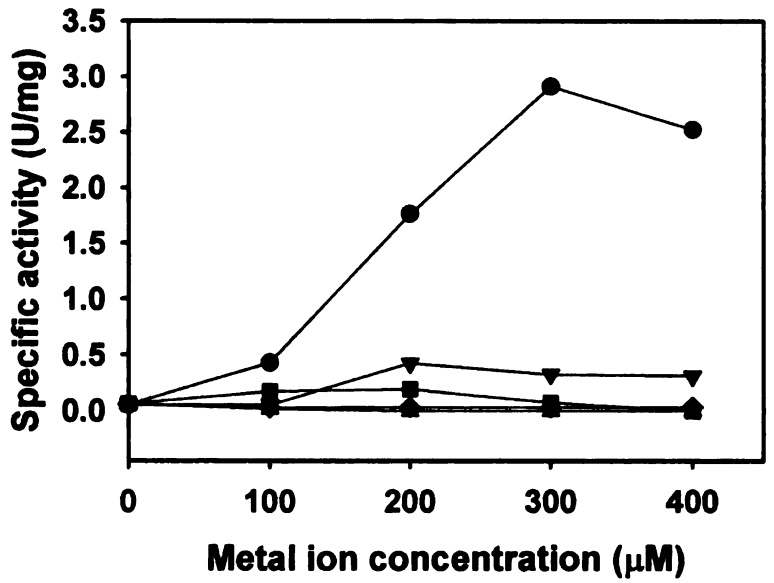

Figure 5. Effects of varied metal ion concentrations on in vitro activation of recombinant *B. subtilis* urease. The *E. coli* transformant (pURE91) was cultured in the absence of nickel, and the cell extracts containing *B. subtilis* apourease were incubated under standard activation conditions with the indicated concentrations of metal salts: $NiCl_2$ (●), $MnCl_2$ (▼), $ZnCl_2$ (■), and $MgCl_2$ (▲) and $CoCl_2$ (♦). After 90 min, cell extracts were prepared and urease activities were determined.

preparations of the partially purified (approximately 85% homogeneous) *B. subtilis* urease were subjected to ICP metal analysis, and 0.13 - 0.29 moles of Ni and 0.063 - 0.070 moles of Zn were detected per mole of αβγ unit, with no significant levels of other metal ions observed. During sample preparation approximately 60% of the activity was lost during exchange of protein from buffer to water, which may represent partial loss of nickel ions. These results confirm that *B. subtilis* urease is a nickel-containing enzyme, but also show that most of the sample is the apoprotein.

Direct comparison of the activities resulting from recombinant expression of *B. subtilis ureABC* and *K. aerogenes ureABC*. The detection of urease activity in *E. coli* cells expressing *B. subtilis ureABC* prompted us to reevaluate the capacity of recombinant cells containing only *K. aerogenes ureABC* to synthesize active urease. Prior studies had suggested that the *K. aerogenes* structural genes by themselves were ineffective in producing functional enzyme (28), but very low levels of activity would not have been detected. In order to conduct a direct comparison of the two systems, two plasmids (pURE93 and pKAU602) were constructed to contain only the UreABC coding regions of *B. subtilis* and *K. aerogenes*, respectively, using the same expression vector and cloning strategy. The plasmids were transformed into C41(DE3) *E. coli* hosts and expressed using the same induction conditions. As illustrated in Figure 6, *B. subtilis ureABC* was expressed at higher levels than *K. aerogenes ureABC* and, in both cases, the UreA subunit was overproduced compared to the other two subunits. The excess UreA synthesis may be due to

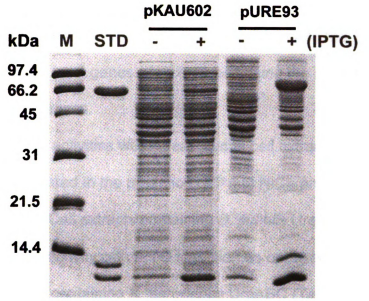

Figure 6. Direct comparison of the expression of *K. aerogenes ureABC* and *B. subtilis ureABC* from pET-42b derived vectors. Cultures of *E. coli* C41(DE3) cells carrying pKAU602 or pURE93 were induced with 0.5 mM IPTG and the cell extracts were analyzed by denaturing polyacrylamide gel. Lanes: 1, molecular weight markers; 2, *K. aerogenes* urease standard; 3 and 4, cell extracts containing *K. aerogenes* UreABC; 5 and 6, cell extracts containing *B. subtilis* UreABC.

the more efficient ribosome binding site provided by the expression vector for *ureA* than the intrinsic ribosome binding sites in the DNA sequences of the other two genes. In contrast, excessive UreA synthesis was not observed when using pURE91 to form the *B. subtilis* urease or pKK17 to make the *K. aerogenes* urease, where the *ureA* genes are expressed using the ribosome binding sites in the genomic sequences.

The urease activities were measured in cell extracts of the two *E. coli* transformants cultured in the presence of 7 mM $NiCl_2$ and the presence or absence of IPTG. Cell extracts containing *B. subtilis* UreABC exhibited ~ 9 U/mg protein of specific activity with IPTG induction as opposed to ~ 0.4 U/mg protein in the cell extracts containing *K. aerogenes* UreABC (Table 3), in approximate correspondence to the amount of UreC present in the extracts as observed in Figure 6. Although the urease activity found in the cells harboring pKAU602 was relatively low compared to the activity measured from the cells containing pURE93, this result overturns prior dogma about the requirement for urease apoprotein activation by accessory proteins.

To investigate the in vitro activation properties of *K. aerogenes* UreABC, activation was performed using the cell extracts from the transformant cells cultured in the absence of supplemental nickel. No activity was detected prior to activation, consistent with the ability of TB medium to sequester trace levels of the required metal ion. In vitro activation of this sample with 300 μM $NiCl_2$ resulted in specific urease activity of ~ 0.8 U/mg of protein (Table 3).

TABLE 3. Urease activity in recombinant E. coli C41(DE3) cell extracts containing the indicated plasmids grown in the presence of 7 mM nickel or grown without supplemental nickel ions and subjected to activation conditions.

Culture	Specific activity (μmol of urea per min per mg)	
	- IPTG	+ IPTG
pKAU602	0.0463	0.438
pURE93	0.756	9.11
	- activation	+ activation
pKAU602	ND[a]	0.838
pURE93	0.144	1.344

[a] Not detected

Complementation studies with urease accessory genes. Co-expression of *K. aerogenes ureDABC* with *K. aerogenes ureEFG* using compatible vectors in *E. coli* cells is known to significantly enhance urease activity in the cell extracts (28); thus, I tested whether co-expression of *ureEFGD* from *K. aerogenes* or *B. pasteurii* with *B. subtilis ureABC* would affect the level of this urease activity. The *B. subtilis* urease subunits share high sequence identity with those of both other microorganisms (e.g., 69 % identity to UreA, 48 % UreB, and 61 % to UreC of *K. aerogenes* urease) so cross-reactivity could reasonably be expected. At the same time, I confirmed that *K. aerogenes ureDEFG* complements *K. aerogenes ureABC*.

Plasmid pACT-ABCdel (containing *ureDEFG* of *K. aerogenes* under control of the *tac* promoter) was co-transformed with pURE93 (encoding *B. subtilis ureABC*) or pKAU602 (containing *K. aerogenes ureABC*) into the *E. coli* host. Gene expression from each of the separate vectors was clearly visible during IPTG induction (Figure 7). While the compatible vectors containing the cognate *K. aerogenes* genes yielded high levels of urease activity (much greater than for pKAU602 alone), co-expression of pURE93 and pACT-ABCdel did not enhance the urease activity over that measured for pURE93 alone (Table 4). Rather, the observed urease activity decreased in the co-transformant as opposed to the transformant containing pURE93 alone, perhaps due to reduced efficiency of expression from two plasmids in the same host versus expression from a single plasmid. This decrease in urease activity also occurred for co-transformation with pACT3 as a control. Similarly, the *B. pasteurii* accessory

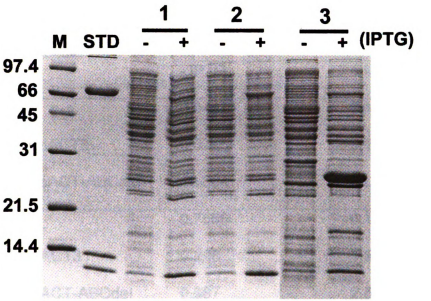

Figure 7. Coexpression of *ureABC* with urease accessory genes. Cultures of *E. coli* cotransformants were induced with 1 mM IPTG in the presence of 5 mM $NiCl_2$: 1, pKAU602 + pACT-ABCdel ; 2, pURE93 + pACT-ABCdel; 3. pURE93 + pACT-BpEFGD. Lanes: 1, molecular weight markers; 2, *K. aerogenes* urease standard. Predicted sizes for *K. aerogenes* urease: UreA (11.1 kDa), UreB (11.7 kDa), UreC (60.3 kDa), UreE (17.6 kDa), UreF (25.2 kDa), UreG (21.9 kDa), and UreD (29.8 kDa); for *B. subtilis* urease: UreA (11.5 kDa), UreB (13.6 kDa), and UreC (61.2 kDa); for *B. pasteurii* accessory proteins: UreE (17.4 kDa), UreF (22.97 kDa), UreG (23.1 kDa), UreD (29.3 kDa).

TABLE 4. Urease activity from *E. coli* cotransformants grown in medium containing 5 mM $NiCl_2$

Culture	Specific activity (μmol of urea per min per mg)	
	- IPTG	+ IPTG
pKAU602	0.0463	0.4129
pKAU602 + pACT3	0.0765	0.114
pKAU602 + pACT-ABCdel	12.684	70.377
pURE93	0.7556	9.114
pURE93 + pACT3	0.298	1.59
pURE93 + pACT-ABCdel	0.987	2.5
pURE93 + pACT-BpEFGD	0.066	0.154

proteins failed to complement the *B. subtilis* structural genes (Table 4). Unlike the *K. aerogenes* accessory genes, the *B. pasteurii* accessory genes exhibited high-level expression from the vector, which might have resulted in compensatory reductions in expression from pURE93; thus, resulting in lower urease activity than seen with other experimental groups. In summary, the *B. subtilis* urease subunits did not interact with heterologous urease accessory proteins from *K. aerogenes* or *B. pasteurii* as measured by changes in activation of the *B. subtilis* urease apoprotein.

DISCUSSION

Urease activity in the absence of known urease accessory genes.

The *B. subtilis* genome contains no known urease-related genes beyond those encoding the three urease subunits (20), yet these cells produce active enzyme. Although the level of urease activity in these cells is quite low, I confirmed that the activity is sufficient to allow growth on urea as sole nitrogen source. Complementary studies by other investigators have shown that *B. subtilis* loses its ability to utilize urea as a nitrogen source when *ureC* is inactivated (14). Significantly, expression of the three *B. subtilis* urease genes in recombinant *E. coli* C41(DE3) cells (which lack homologues to any of the known urease-related genes) results in low levels of urease activity. Furthermore, trace levels of urease activity were detected in *E. coli* cells containing the genes encoding the *K.*

aerogenes urease subunits. I conclude that active urease can be produced, albeit with low efficiency, in the absence of the *ureDEFG* accessory genes.

Properties of recombinant *B. subtilis* urease. Recombinant *B. subtilis* urease is produced primarily as an apoprotein, even when cells are grown in near-toxic concentrations of nickel ion. The amount of nickel present in the protein roughly correlates with the observed activity level of the recombinant enzyme. For example, an average of 0.2 nickel per $\alpha\beta\gamma$ unit corresponds to 0.1 nickel at each of the two metal sites of the presumed dinuclear center; thus, only ~10 % of each active site would possess both of the nickel ions required for activity. The observed specific activity the enriched urease is the same order of magnitude percentage when compared to fully active *K. aerogenes* enzyme (2,500 U/mg protein)(41).

The urease present in recombinant cell extracts is activated to only a small extent by using the standard in vitro activation procedure developed for the purified *K. aerogenes* urease apoprotein. Efforts to modify the activation conditions (varying pH, bicarbonate concentration, or nickel ion concentration) did not result in higher levels of activation. The low efficiency of in vitro activation is not surprising when compared with other systems. For example, only ~15% of *K. aerogenes* urease apoprotein is activated under these conditions even though metal quantification and bicarbonate labeling studies show stoichiometric lysine carbamylation and incorporation of a full complement of nickel (30, 31). In a similar manner, only a small percentage of *B. subtilis* urease apoprotein is activated by this approach.

A property unique to the *B. subtilis* enzyme is its lability to high concentrations of salts. This instability, which confounded efforts to purify the enzyme, is not alleviated by inclusion of glycerol or other additives. In the presence of high concentrations of KCl the UreB and UreC subunits were shown to precipitate, with UreA remaining soluble.

Effects of accessory proteins on recombinant *B. subtilis* urease activity. Sequences of genes encoding the urease subunits are highly conserved across species, while the accessory genes exhibit much lower sequence conservation (25, 26); nevertheless, I was unable to find any convincing homologues to *ureD*, *ureE*, *ureF*, or *ureG* in the *B. subtilis* genome. Our efforts to enhance recombinant *B. subtilis* urease activity by complementing these structural genes with the known accessory genes from either *K. aerogenes* or *B. pasteurii* were unsuccessful. This result suggests that, despite the high similarity in sequences of the urease subunits among these species, there is sufficient disparity to prevent the formation of a functional activation complex between the heterologous accessory proteins and the *B. subtilis* apoprotein. It is possible, however, that endogenous *E. coli* components may facilitate the observed synthesis of low levels of active urease expressed from *B. subtilis* or *K. aerogenes ureABC*. One possibility for a facilitator protein is SlyD, known to assist in activation of nickel-containing hydrogenase (46). Countering the participation of SlyD in these constructs are prior studies showing no effect when the intact or *ureE*-deleted *K. aerogenes* urease gene cluster was transformed into *slyD* versus wild-type *E. coli* cells (7). To summarize, trace levels of

recombinant urease are activated in *E. coli* without the participation of known urease accessory genes.

Evidence for the presence of novel accessory proteins in *B. subtilis*. Although *B. subtilis* lacks homologues to the established urease accessory genes, I cannot rule out the presence of one or more non-homologous accessory genes located at a locus (loci) separated from the subunit genes. Two lines of evidence provide potential support for the existence of such a gene(s). First, the urease activity in *B. subtilis* is comparable to that in the recombinant *E. coli* cells, despite the vast overproduction of urease protein in the latter cultures. This result is consistent with an increased efficiency of urease activation in *B. subtilis* that could arise from increased intracellular nickel or bicarbonate ion concentrations, folding issues in the heterologous host, or the presence of a novel accessory gene(s). Elevated intracellular nickel ion concentrations are possible if *B. subtilis* possesses an active nickel uptake system. Nickel uptake has not been examined in this microorganism, but its genome contains homologues of genes encoding the HoxN nickel permease and MgtA, ZntA, and MgtE cation transporters. High intracellular nickel ion concentrations also could develop if *B. subtilis* lacks a nickel export system; by contrast, *E. coli* possesses the *rcnA* nickel export system that is induced in the presence of elevated nickel ion concentrations and serves to maintain lower intracellular levels of this metal ion despite near toxic levels in the medium (34). Elevated intracellular concentrations of bicarbonate ion are possible if *B. subtilis* possesses a mechanism to concentrate carbon dioxide similar to that found in chloroplasts (22). The lack of any clear

bicarbonate concentrating system in the genomic sequence is compatible with the possibility that *B. subtilis* possesses an unidentified facilitator gene.

The second line of evidence for a novel urease accessory gene in *B. subtilis* is the lack of enhanced urease activity in *B. subtilis* cells overexpressing recombinant *ureABC*. These cells are expected to contain nickel and bicarbonate concentrations equivalent to those of the wild-type *B. subtilis* cells, and there are no concerns about the protein folding machinery synthesizing heterologous proteins; yet, a much lower proportion of urease is activated in these cells. One explanation to account for these results is that an unidentified accessory protein assists in urease activation and functions in a stoichiometric manner. Further studies are required to examine whether *B. subtilis* possesses one or more unidentified accessory gene(s).

Other urealytic systems lacking one or more accessory proteins. Over 200 microbial genomes have been sequenced, and approximately 20 % contain homologues to *ureC*. Additional sequence information is available from targeted sequencing efforts to characterize the urease gene clusters of numerous microorganisms. For most bacteria, the structural genes (*ureABC*) are clustered with the accessory genes (*ureDEFG*; with *ureD* sometimes referred to as *ureH*) in various closely spaced arrangements (24, 25). In selected microorganisms, however, the urease genes are interrupted by long intervening sequences. For example *Agrobacterium tumefaciens* (GenBank accession no.: AE007869) contains all of the urease genes (*ureABCDEFG*), but six open reading frames (ORFs) encoding short polypeptides (85 to 221 amino acids in

length) of unknown function interrupt the gene cluster. Similarly, *ureDABC* and *ureEFG* of *Pseudomonas aeruginosa* PAO1 (GenBank: AE004091) and *Pseudomonas syringae* pv. tomato str. (GenBank: AE016853) are separated by more than 15,000 base pairs (with an additional one or two ORFs between *ureA* and *ureB*, respectively). Even more striking are the situations for *Synecocystis sp.* PCC 6803 (GenBank: BA000022) and *Thermosynechococcus elongatus* BP-1 (GenBank: BA000039) where the individual urease genes (*ureABCDEFG*) are dispersed throughout the entire genome without forming any gene clusters. These microorganisms face the difficulty of coordinating expression from widely dispersed genes, if indeed all of these genes are required to synthesize active urease.

Of greater relevance to the *B. subtilils* system are cases where one or more urease accessory genes are missing in a urea-degrading microorganism. As shown by the examples described above, one cannot conclude that an accessory gene is absent using only the sequence of a urease gene cluster; rather, the entire genome must be examined. The urease gene cluster of *Mycobacterium tuberculosis* Erdman strain (ATCC 35801) contains only *ureABCFG*, yet the bacterium synthesizes a urease that when purified has low activity (101 U/mg protein) (11). It is possible that the missing genes are elsewhere on the chromosome in this microorganism or that both *ureD* and *ureE* are absent. In contrast, the genomes of *M. tuberculosis* strain CDC1551 (GenBank accession no.: AE000516), *M. tuberculosis* strain H37Rv (GenBank: AL123456), and *M. bovis* strain AF2122/97 (GenBank: BX248333) contain

ureABCFG plus *ureD* and lack only *ureE*. Similarly, the genomes of *Candidatus Blochmannia floridanus* (GenBank: BX248583), *Streptomyces avermitilis* MA-4680, *Streptomyces coelicolor* A3(2), *Bradyrhizobium japonicum*, *Rhodopseudomonas palustris* CGA009, and *Nocardia farcinica* appear to lack homologues to *ureE*. According to the complete microbial genome data available up to date, *B. subtilis* is the only organism that synthesizes a functional urease in the absence of any known accessory genes in its genome.

Activation of non-urease dinuclear hydrolases. In contrast to the elaborate set of accessory proteins required for synthesis of most ureases, several structurally-related dinuclear hydrolases are spontaneously activated without any accessory proteins. For example, phosphotriesterase (5), dihydroorotase (40), isoaspartyl dipeptidase (39), and three different hydantoinases (1, 2, 10) all contain active sites that closely resemble that of urease, with a carbamylated lysine residue bridging two metal ions (typically zinc for these enzymes). No genetic or biochemical evidence has been reported to implicate the need for accessory proteins during biosynthesis of these enzymes.

I suggest that the simple urease system of *B. subtilis* provides a link for understanding the differences in activation of the above enzymes and that of the typical urease systems. Thus, CO_2 can modify the appropriate lysine residues in the apoproteins of selected dinuclear hydrolases and the carbamylated residue can bind metal ions without the participation of accessory proteins; however, the efficiency of this process is quite low when using nickel ions rather than zinc ions. Accessory proteins are used to enhance the efficiency of activation by a still

poorly understood process in which metal incorporation is coupled to GTP hydrolysis. Of related interest, the activation of nickel-containing hydrogenases, carbon monoxide dehydrogenase, and acetyl-CoA decarbonylase/synthase also requires accessory genes for efficient metallocenter assembly (27).

REFERENCES

1. **Abendroth, J., K. Niefind, O. May, M. Siemann, C. Syldatk, and D. Schomburg.** 2002. The structure of L-hydantoinase from *Arthrobacter aurescens* leads to an understanding of dihydropyrimidinase substrate and enantio specificity. Biochemistry **41:**8589-8597.

2. **Abendroth, J., K. Niefind, and D. Schomburg.** 2002. X-ray structure of a dihydropyrimidinase from *Thermus* sp. at 1.3 Å resolution. J. Molec. Biol. **320:**143-156.

3. **Atkinson, M. R., and S. H. Fisher.** 1991. Identification of genes and gene products whose expression is activated during nitrogen-limited growth in *Bacillus subtilis*. J. Bacteriol. **173:**23-27.

4. **Benini, S., W. R. Rypniewski, K. S. Wilson, S. Miletti, S. Ciurli, and S. Mangani.** 1999. A new proposal for urease mechanism based on the crystal structures of the native and inhibited enzme from *Bacillus pasteurii*: why urea hydrolysis costs two nickels. Structure **7:**205-216.

5. **Benning, M. M., J. M. Kuo, F. M. Raushel, and H. M. Holden.** 1995. Three-dimensional structure of the binuclear metal center of phosphotriesterase. Biochemistry **34:**7973-7978.

6. **Bradford, M. M.** 1976. A rapid and sensitive method for the quantitation of microgram quantities of protein utilizing the principle of protein-dye binding. Anal. Biochem. **72:**248-254.

7. **Brayman, T. G., and R. P. Hausinger.** 1996. Purification, characterization, and functional analysis of a truncated *Klebsiella aerogenes* UreE urease accessory protein lacking the histidine-rich carboxyl terminus. J. Bacteriol. **178:**5410-5416.

8. **Britton, R. A., P. Eichenberger, J. E. Gonzalez-Pastor, P. Fawcett, R. Monson, R. Losick, and A. D. Grossman.** 2002. Genome-wide analysis of the stationary-phase sigma factor (sigma-H) regulon of *Bacillus subtilis*. J. Bacteriol. **184:**4881-4890.

9. **Chang, Z., J. Kuchar, and R. P. Hausinger.** 2004. Chemical crosslinking and mass spectrometric identification of sites of interaction for UreD, UreF, and urease. J. Biol. Chem. **279:**15305-15313.

10. **Cheon, Y.-H., H.-S. Kim, K.-H. Han, J. Abendroth, K. Niefind, D. Schomburg, J. Wang, and Y. Kim.** 2002. Crystal structure of D-

hydantoinase from *Bacillus stearothermophilus*: insight into the stereochemistry of enantioselectivity. Biochemistry **41**:9410-9417.

11. **Clemens, D. L., B.-Y. Lee, and M. A. Horwitz.** 1995. Purification, characterization, and genetic analysis of *Mycobacterium tuberculosis* urease, a potentially critical determinant of host-pathogen interaction. J. Bacteriol. **177**:5644-5652.

12. **Colpas, G. J., T. G. Brayman, L.-J. Ming, and R. P. Hausinger.** 1999. Identification of metal-binding residues in the *Klebsiella aerogenes* urease nickel metallochaperone, UreE. Biochemistry **38**:4078-4088.

13. **Colpas, G. J., and R. P. Hausinger.** 2000. In vivo and in vitro kinetics of metal transfer by the *Klebsiella aerogenes* urease nickel metallochaperone, UreE. J. Biol. Chem. **275**:10731-10737.

14. **Cruz-Ramos, H., P. Glaser, L. V. Wray, Jr., and S. H. Fisher.** 1997. The *Bacillus subtilis ureABC* operon. J. Bacteriol. **179**:3371-3373.

15. **Dykxhoorn, D. M., R. St. Pierre, and T. Linn.** 1996. A set of compatible *tac* promoter expression vectors. Gene **177**:133-136.

16. **Ha, N.-C., S.-T. Oh, J. Y. Sung, K.-A. Cha, M. H. Lee, and B.-H. Oh.** 2001. Supramolecular assembly and acid resistance of *Helicobacter pylori* urease. Nature Structure Biology **8**:505-509.

17. **Hausinger, R. P., and P. A. Karplus.** 2001. Urease, p. 867-879. *In* K. Wieghardt, R. Huber, T. L. Poulos, and A. Messerschmidt (ed.), Handbook of Metalloproteins. John Wiley & Sons, Ltd., West Sussex, U.K.

18. **Jabri, E., M. B. Carr, R. P. Hausinger, and P. A. Karplus.** 1995. The crystal structure of urease from *Klebsiella aerogenes*. Science **268**:998-1004.

19. **Kim, S. D., and R. P. Hausinger.** 1994. Genetic organization of the recombinant *Bacillus pasteurii* urease genes expressed in *Escherichia coli*. J. Microbiol. Biotech. **4**:108-112.

20. **Kunst, F., N. Ogasawara, I. Moszer, A. M. Albertini, G. Alloni, V. Azevedo, M. G. Bertero, P. Bessières, A. Bolotin, S. Borchert, R. Borriss, L. Boursier, A. Brans, M. Braun, S. C. Brignell, S. Bron, S. Brouillet, C. V. Bruschi, B. Caldwell, V. Capuano, N. M. Carter, S.-K. Choi, J.-J. Codani, I. F. Connerton, N. J. Cummings, R. A. Daniel, F. Denizot, K. M. Devine, A. Düsterhöft, S. D. Ehrlich, P. T. Emmerson, K. D. Entian, J. Errington, C. Fabret, E. Ferrari, D. Foulger, C. Fritz, M. Fujita, Y. Fujita, S. Fuma, A. Galizzi, N. Galleron, S.-Y. Ghim, P.**

Glaser, A. Goffeau, E. J. Golightly, G. Grandi, G. Guiseppi, B. J. Guy, K. Haga, J. Haiech, C. R. Harwood, A. Hènaut, H. Hilbert, S. Holsappel, S. Hosono, M.-F. Hullo, M. Itaya, L. Jones, B. Joris, D. Karamata, Y. Kasahara, M. Klaerr-Blanchard, C. Klein, Y. Kobayashi, P. Koetter, G. Koningstein, S. Krogh, M. Kumano, K. Kurita, A. Lapidus, S. Lardinois, J. Lauber, V. Lazarevic, S.-M. Lee, A. Levine, H. Liu, S. Masuda, C. Mauël, C. Mèdigue, N. Medina, R. P. Mellado, M. Mizuno, D. Moesti, S. Nakai, M. Noback, D. Noone, M. O'Reilly, K. Ogawa, A. Ogiwara, B. Oudega, S.-H. Park, V. Parro, T. M. Pohl, D. Portetelle, S. Porwollik, A. M. Prescott, E. Presecan, P. Pujic, B. Purnelle, et al. 1997. The complete genome sequence of the Gram-positive bacterium *Bacillus subtilis*. Nature **390**:249-256.

21. **Laemmli, U. K.** 1970. Cleavage of structural proteins during the assembly of the head of bacteriophage T4. Nature (London) **227**:680-685.

22. **Leegood, R. C.** 2002. C_4 photosynthesis: principles of CO_2 concentration and prospects for its introduction into C_3 plants. J. Exper. Bot. **53**:581-590.

23. **Miroux, B., and J. E. Walker.** 1996. Over-production of proteins in *Escherichia coli*: mutant hosts that allow synthesis of some membrane protein and globular proteins at high levels. J. Molec. Biol. **260**:289-298.

24. **Mizuki, T., M. Kamekura, S. DasSarma, T. Fukushima, T. Usami, Y. Yoshida, and K. Horikoshi.** 2004. Ureases of extreme halophiles of the genus *Haloarcula* with a unique structure of gene cluster. Bioscience, Biotechnology, and Biochemistry **68**:397-406.

25. **Mobley, H. L. T., M. D. Island, and R. P. Hausinger.** 1995. Molecular biology of microbial ureases. Microbiol. Rev. **59**:451-480.

26. **Moncrief, M. B. C., and R. P. Hausinger.** 1996. Nickel incorporation into urease, p. 151-171. *In* R. P. Hausinger, G. L. Eichhorn, and L. G. Marzilli (ed.), Mechanisms of Metallocenter Assembly. VCH Publishers, New York.

27. **Mulrooney, S. B., and R. P. Hausinger.** 2003. Nickel uptake and utilization by microorganisms. FEMS Microbiol. Rev. **27**:239-261.

28. **Mulrooney, S. B., and R. P. Hausinger.** 1990. Sequence of the *Klebsiella aerogenes* urease genes and evidence for accessory proteins facilitating nickel incorporation. J. Bacteriol. **172**:5837-5843.

29. **Mulrooney, S. B., S. K. Ward, and R. P. Hausinger.** 2005. Purification and properties of the Klebsiella aerogenes UreE metal-binding domain, a functional metallochaperone of urease. J. Bacteriol. **187**:3581-3585.

30. **Park, I.-S., and R. P. Hausinger.** 1996. Metal ion interactions with urease and UreD-urease apoproteins. Biochemistry **35:**5345-5352.

31. **Park, I.-S., and R. P. Hausinger.** 1995. Requirement of carbon dioxide for in vitro assembly of the urease nickel metallocenter. Science **267:**1156-1158.

32. **Pearson, M. A., L. O. Michel, R. P. Hausinger, and P. A. Karplus.** 1997. Structure of Cys319 variants and acetohydroxamate-inhibited *Klebsiella aerogenes* urease. Biochemistry **36:**8164-8172.

33. **Pearson, M. A., I.-S. Park, R. A. Schaller, L. O. Michel, P. A. Karplus, and R. P. Hausinger.** 2000. Kinetic and structural characterization of urease active site variants. Biochemistry **39:**8575-8584.

34. **Rodrigue, A., G. Effantin, and M. A. Mandrand-Bethelot.** 2005. Identification of *rcnA* (*yohM*), a nickel and cobalt resistance gene in *Escherichia coli*. J. Bacteriol. **187:**2912-2916.

35. **Sambrook, J., E. F. Fritsch, and T. Maniatis.** 1989. Molecular cloning: a laboratory manual, 2nd ed. Cold Spring Harbor Laboratory, Cold Spring Harbor, NY.

36. **Sheridan, L., C. M. Wilmont, K. D. Cromie, P. van der Logt, and S. E. V. Phillips.** 2001. Crystallization and preliminary X-ray structure determination of jack bean urease with a bound antibody fragment. Acta Crystallographa **D58:**374-376.

37. **Soriano, A., G. J. Colpas, and R. P. Hausinger.** 2000. UreE stimulation of GTP-dependent urease activation in the UreD-UreF-UreG-urease apoprotein complex. Biochemistry **39:**12435-12440.

38. **Soriano, A., and R. P. Hausinger.** 1999. GTP-dependent activation of urease apoprotein in complex with the UreD, UreF, and UreG accessory proteins. Proc. Natl. Acad. Sci. USA **96:**11140-11144.

39. **Thoden, J. B., R. Marti-Arbona, F. M. Raushel, and H. M. Holden.** 2003. High-resolution x-ray structure of isoaspartyl dipeptidase from *Escherichia coli*. Biochemistry **42:**4874-4882.

40. **Thoden, J. B., G. N. Phillips, Jr., T. M. Neal, F. M. Raushel, and H. M. Holden.** 2001. Molecular structure of dihydroorotase: a paradigm for catalysis through use of a binuclear metal center. Biochemistry **40:**6989-6997.

41. **Todd, M. J., and R. P. Hausinger.** 1989. Competitive inhibitors of *Klebsiella aerogenes* urease. Mechanisms of interaction with the nickel active site. J. Biol. Chem. **264:**15835-15842.

42. **Todd, M. J., and R. P. Hausinger.** 1987. Purification and characterization of the nickel-containing multicomponent urease from *Klebsiella aerogenes*. J. Biol. Chem. **262:**5963-5967.

43. **Vasantha, N., and E. Freese.** 1980. Enzyme changes during *Bacillus subtilis* sporulation caused by deprivation of guanine nucleotides. J. Bacteriol. **144:**1119-1125.

44. **Weatherburn, M. W.** 1967. Phenol-hypochlorite reaction for determination of ammonia. Anal. Chem. **39:**971-974.

45. **Yamaguchi, K., S. Koshino, F. Akagi, M. Suzuki, A. Uehara, and S. Suzuki.** 1997. Structures and catalytic activities of carboxylate-bridged dinickel(II) complexes as models for the metal center of urease. J. Am. Chem. Soc. **119:**5752-5753.

46. **Zhang, J. W., G. Butland, J. F. Greenblatt, A. Emili, and D. B. Zamble.** 2005. A role for SlyD in the *Escherichia coli* hydrogenase biosynthetic pathway. J. Biol. Chem. **280:** 4360-4366.

CHAPTER 3

Screening of *Bacillus subtilis* Genome for Novel Non-homologous Accessory Genes

ABSTRACT

The *Bacillus. subtilis* genome contains no known urease accessory genes, in contrast to the situation found in other ureolytic microorganisms, yet this organism exhibits a low level of urease activity which is sufficient for growth on urea as sole nitrogen source. In this study, a *B. subtilis* genomic library was created and used to screen novel non-homologous accessory gene(s) or potential urease enhancing factors by coexpressing the library and the *B. subtilis* urease structural gene cluster in an *E. coli* host grown on urease indicator agar. Of 5,544 cotransformants screened, 13 isolates exhibited a rapid color change of the indicator medium presumably due to increased pH which could arise from elevated urease activity. Plasmids from the positive clones were isolated and sequenced to identify the genes responsible for the enhanced urease activity. Surprisingly, however, none of the positive isolates showed increased urease activity when the activities were quantitatively determined by phenol-hypochlorite urease assay. Although the basis of these results is not well understood, I hypothesize that these isolates exhibit reduced acid production, due to direct or indirect effects of the exogenous *B. subtilis* gene products on the metabolism of the host cells, so that basal levels of *B. subtilis* urease activity increase the pH around the cells more rapid and result in a color change of the pH indicator.

INTRODUCTION

The *Bacillus. subtilis* genome lacks homologues to the established urease accessory genes; nevertheless, this organism can produce active enzyme and grow on urea as sole nitrogen source (4, 6). It is not yet clear, however, whether the organism has unidentified non-homologous accessory gene(s) located at a locus (loci) separated from the subunit genes or if it lacks accessory genes in its genome so that its urease activates spontaneously. Two observations from previous studies (Chapter 2) support the possible existence of non-homologous accessory gene(s). First, the activity in *B. subtilis* is comparable to that in the recombinant *E. coli* cells, despite the vast overproduction of urease protein in the latter cultures. Second, *B. subtilis* cells overexpressing recombinant *B. subtilis ureABC* lack enhanced urease activity. These cells are expected to contain Ni^{2+} and bicarbonate concentrations equivalent to those of the non-recombinant *B. subtilis* cells and the folding machinery acts on homologous proteins; yet, a much lower proportion of urease is activated. This led me to hypothesize the existence of unidentified accessory protein(s) that assist in urease activation in a stoichiometric manner.

In this chapter, I attempted to identify non-homologous accessory gene(s) or potential urease enhancing factor(s) by screening the *B. subtilis* genomic library using the coexpression approach with the *B. subtilis* urease gene cluster.

MATERIALS AND METHODS

Bacterial strains and culture conditions. *E. coli* DH5α cells were used as host for coexpression of *B. subtilis* urease and genomic DNA library. *E. coli* *ΔcarB* mutant and wild type strains (BW25113) were purchased from Nara Institute of Science and Technology (Nara, Japan). Urease activities of the *E. coli* cotransformants were monitored on urease indicator agar (7), which contained the following per 900 ml: 4 g of yeast extract, 4 g of peptone, 0.34 g of NaH_2PO_4, 1.03 g of $Na_2HPO_4 \cdot 7H_2O$, 5 g of NaCl, 0.9 g of KH_2PO_4, 1.1 g of K_2HPO_4, and 15 g of agar. After autoclaving, a 100 ml filter-sterilized solution containing 0.9 g of glucose, 6 g of urea, and 0.035 g of phenol red, 1 mM $NiCl_2$, and appropriate antibiotics was added. The pH of uninoculated medium was adjusted so that the color was light orange (~ pH 6.9). The cotransformants were grown at 37 °C overnight (~ 17 hr) before determination of urease activity. For preparation of cell extracts for phenol-hypochlorite urease assay, the cotransformants were cultured in Terrific Broth (TB, Fisher Biotech) supplemented with appropriate antibiotics at 37 °C to an OD_{600} ~ 0.4, induced with 0.5 mM isopropyl β-D-thiogalactopyranoside (IPTG, Roche) plus supplementary $NiCl_2$ (5 mM), and harvested after 14-16 hr.

Construction of pACT-BsABC. All restriction digestions and DNA manipulations were performed by following standard procedures (11). Primers were synthesized at Integrated DNA Technologies, Inc. (Coralville, Iowa). To construct pACT-BsABC, the DNA fragment covering the coding region of *B.*

subtilis urease was amplified by using pURE91 as a template and the following primers: pACT-BsABC-For (5'-CGCGGATCCGGCTGATGAAACGGCATG CCGCTT-3'; the *Bam*HI restriction site is underlined), and pACT-BsABC-Rev (5'-CTAGTCTAGATAGTCAATAGAACGGCCGGATGCACTC-3'; an *Xba*I restriction site is underlined). The resulting fragment was digested with *Bam*HI and *Xba*I, and cloned into similarly digested pACT3 (5) to yield pACT-BsABC. The sequence was verified by sequencing throughout the entire coding region.

Construction of *B. subtilis* genomic library. The *B. subtilis* genomic library was constructed, essentially following the procedures described (10). Genomic DNA was isolated from *B. subtilis* SF10 (Wild type, SMY derivative) by using the GenElute Bacterial Genomic DNA kit (Sigma), and partially digested with *Sau*3AI. After size fractionation by agarose gel electrophoresis, DNA fragments ranging from 2.5 kb to 5 kb were isolated. The 5' sticky ends generated by *Sau*3AI treatment were partially filled in by using Klenow DNA polymerase (New England Biolabs) and dATP plus dGTP (Invitrogen). *Sal*I-digested pBluescript II SK(-) vector was similarly partially filled in with dTTP and dCTP. The genomic and vector DNA were ligated in a 1:1 ratio. For the initial analysis of the library, 3 µl of the ligation mixture (containing 36 ng vector and 36 ng genomic DNA) was transformed into Max efficiency *E. coli* DH5α (Invitrogen). Transformants were selected on LB agar medium supplemented with ampicillin, IPTG, and 5-bromo-4-chloro-3-indolyl-β-D-galactoside (X-gal) by following the standard procedures (11). Of the 2.04×10^4 ampicillin-resistant colonies, 89.2% were white, indicating that they carried recombinant plasmids. Based on the

average insert size (3.5 kb) and the known size of the *B. subtilis* genome (4.2 Mb), the number of clones to be screened (N) was calculated by using the following equation where P is % probability of isolating an individual sequence, l is the size of the average cloned fragment in base pairs, and G is the size of the target genome in base pairs (1).

$$N = \ln (1-P)/ \ln [1- (l/G)]$$

For 99 % probability of including the desired fragment, about 5554 colonies needed to be screened.

Preparation of electrocompetent DH5α containing pACT-BsABC and electroporation. *E. coli* DH5α containing pACT-BsABC was subjected to standard procedures to make the cells electrocompetent (1). Transformation efficiency of the electrocompetent cells was estimated to be ~ 1 x 10^9, using control vector (pUC19). Electrotransformation was carried out by using a Gene Pulser Xcell™ Electroporation system (Biorad). Briefly, 2 µl of *B. subtilis* genomic library was mixed with 40 µl of the electrocompetent cells in a 0.2 cm cuvette, pulsed at 2.5 kV, and incubated in SOC medium (Invitrogen) for 1 hour before plating.

Screening of cotransformants on urease indicator agar. The *E. coli* cotransformants harboring pACT-BsABC and the genomic library were screened for colonies that increased the medium pH when grown on urease indicator agar. As the pH of urease indicator medium rises, presumably due to ammonia production by urease activity, the medium immediately surrounding the colonies changes color from light orange to red. Urease activity-negative colonies at the

time of determination (~ 17 hr after plating) change the color of the medium to yellow by acid production due to consumption of glucose by a combination of respiration and mixed-acid fermentation. *E. coli* DH5α carrying pACT-BsABC and pBluescript served as negative control.

Preparation of cell extracts. Cell pellets were resuspended in 20 mM Tris buffer (pH 7.4) containing 150 mM NaCl and 1 mM EDTA (STE buffer), and disrupted by sonication (Branson Sonifier). Intact cells and debris were removed by centrifugation at 10,000 *g* for 20 min at 4 °C.

Phenol-hypochlorite urease assay. Urease activity was measured by quantifying the rate of ammonia release from the hydrolysis of urea by formation of indophenol, which was monitored at 625 nm (13). One unit of urease activity (U) was defined as the amount of enzyme required to hydrolyze 1 μmol of urea per min at 37 °C. The standard assay buffer contained 50 mM HEPES (*N*-2-hydroxyethylpiperazine-*N'*-ethanesulfonic acid; pH 7.8) and 50 mM urea. Protein concentrations were determined by using a commercial assay (Bio-Rad) with bovine serum albumin as the standard (3).

RESULTS AND DISCUSSION

Screening on urease indicator agar. A *B. subtilis* genomic library was constructed and cotransformed into *E. coli* DH5α containing pACT-BsABC (encoding *B. subtilis ureABC*) to identify non-homologous accessory gene(s) or

urease-enhancing factors. The cotransformants were screened for enhanced urease activity on urease indicator agar containing urea and phenol red, where cells containing urease-enhancing factors should exhibit a pH increase leading to a red halo around the colony compared to control cells (pACT-BsABC/control vector). Among 5,544 DH5α (pACT-BsABC/library) cotransformants screened, 36 isolates turned the urease indicator medium red after overnight incubation whereas the control group failed to exhibit this color change even after 2 days (Fig. 1). To eliminate false-positive clones, the 36 potential positive isolates were rescreened on a urease indicator agar to determine reproducibility. Of the 36 isolates, 13 cotransformants yielded consistently positive results, as evidenced by the red color change after overnight incubation.

Sequence characterization of positive clones. Plasmids were isolated from the positive cotransformants and sequenced to identify the DNA fragments inserted from the *B. subtilis* genome. Sequence analysis revealed that 8 out of 12 isolates contained the same DNA fragments covering *yisP*, *yisQ*, and *yisR* (with truncations of *yisP* at the left junction and *yisR* at the right junction). In addition, four separate DNA regions were identified in the other four isolates. The genes identified from the isolates are summarized in Table 1.

Urease activities in cotransfomants contaning *B. subtilis ureABC* and putative urease enhancing factors. To confirm that the color change on the indicator medium (arising from an increased pH around cells from urea hydrolysis) is due to increased urease activity, the phenol-hypochlorite urease assay was performed to measure the urease activities in the control and positive

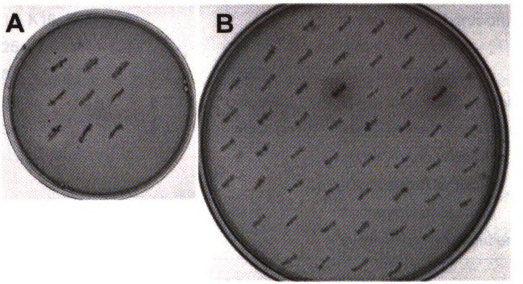

Figure 1. Urease activity on urease indicator agar. A, control *E. coli* DH5α cells (pACT-BsABC/pBluescript). B, a selection of cotransformants (pACT-BsABC/library). Urease activities were monitored by the change of the color of medium around cells after overnight incubation. Two of the cotransformants exhibit a red halo around the colonies, consistent with an increase in the medium pH.

Table 1. Summary of genes identified from the *B.subtilis* genomic library

Isolates	Insert size (kb)	Candidate gene(s)[a]	Function of the genes
K2, K3, K5, K8, K15, K16, K17, and K25	2.6 - 2.9	*yisQ*	putative MATE (Multi-Antimicrobial Extrusion) family protein
K6	1.2	*ybbU*	hypothetical protein
K24	2.7	*spoVR*	stage V sporulation protein R
K34	2.4	*yhzC*, *comK*	*yhzC* – hypothetical protein *comK* – competence transcription factor
K36	3.0	*carA*	carbamoyl phosphate synthetase, small subunit

[a] genes shown in the table are flanked by additional truncated genes at both 5' and 3' ends.

isolates. Surprisingly, none of the positive isolates exhibited enhanced urease activity; rather, they possessed similar levels of activities to control (Table 2). Although the basis of these results is not certain, I hypothesize that these isolates exhibit decreased acid production by direct or indirect effects of the exogenous *B. subtilis* gene products on the metabolism of the host cells so that the basal levels of *B. subtilis* urease activity overcome the weak acid production and lead to a net increase in pH around the cells, resulting in a color change of pH indicator.

Expression of *K. aerogenes* or *B. subtilis* urease in *E. coli carB* knockout mutant. Although none of the isolates exhibited enhanced urease activity, one of the candidate genes, *carA*, was potentially interesting to examine further because *carAB* genes (encoding carbamoyl phosphate synthetase) are required for synthesis of the active center of *E. coli* [NiFe]-hydrogenase (9). Therefore, *K. aerogenes* urease and *B. subtilis* urease gene clusters were transformed into an *E. coli carB* knockout mutant, and the urease activity was assayed in the cell extracts of these transformants to test whether carbamoyl phosphate is involved in the synthesis of active urease. Compared to wild type transformants, urease activity in the *carB* knockout mutant was not significantly different, suggesting that carbamoyl phosphate is not required for the maturation of urease (data not shown).

As described above, the efforts to identify non-homologous accessory gene(s) or urease enhancing factors were not successful. Thus, it still remains unclear whether the urease activation occurs spontaneously in this organism

Table 2. Urease activities in cell extracts of cotransformants containing *B. subtilis* urease and putative urease enhancing factors

Isolates	Candidate gene(s)[a]	Specific activity (U/mg)
Control	-	0.70
K6	*ybbU*	0.34
K8	*yisQ*	0.33
K24	*spoVR*	0.72
K34	*yhzC, comK*	0.46
K36	*carA*	0.15

[a] genes shown in the table are flanked by additional truncated genes at both 5' and 3' ends.

(i.e., without involvement of any accessory proteins) or if the screening just failed to identify the accessory gene(s). Both of these possibilities have precedent in the literature dealing with related metalloenzymes. For example, phosphotriesterase (2) and dihydroorotase (12) contain active sites that resemble that of urease, including a carbamylated lysine residue bridging two zinc ions, but they are spontaneously activated without any accessory proteins. No genetic or biochemical evidence has been reported to suggest the requirement of accessory proteins during biosynthesis of these active enzymes. On the contrary, there are several studies implicating the existence of non-homologous accessory genes functioning in the process of metallocenter assembly. For example, SlyD (14) was shown to assist in nickel insertion during hydrogenase activation although the hydrogenase gene cluster has its own accessory genes dedicated to this step (*hypA* and *hypB*). Similarly, the HypA and HypB proteins functioning in hydrogenase maturation are known to be involved in activation of urease in *H. pylori* (8). Further study will be required to solve the enigma of *B. subtilis* urease activation.

REFERENCES

1. **Ausubel, F., R. Brent, R. Kingston, D. Moore, J. G. Seidman, J. Smith, and K. Struhl.** 1987. *Current protocols in molecular biology.*

2. **Benning, M. M., J. M. Kuo, F. M. Raushel, and H. M. Holden.** 1995. Three-dimensional structure of the binuclear metal center of phosphotriesterase. Biochemistry **34:**7973-7978.

3. **Bradford, M. M.** 1976. A rapid and sensitive method for the quantitation of microgram quantities of protein utilizing the principle of protein-dye binding. Anal. Biochem. **72:**248-254.

4. **Cruz-Ramos, H., P. Glaser, L. V. Wray, Jr., and S. H. Fisher.** 1997. The *Bacillus subtilis ureABC* operon. J. Bacteriol. **179:**3371-3373.

5. **Dykxhoorn, D. M., R. St. Pierre, and T. Linn.** 1996. A set of compatible *tac* promoter expression vectors. Gene **177:**133-136.

6. **Kim, J. K., S. B. Mulrooney, and R. P. Hausinger.** 2005. Biosynthesis of active *Bacillus subtilis* urease in the absence of known urease accessory proteins. J. Bacteriol. **187:**7150-4.

7. **McGee, D. J., C. A. May, R. M. Garner, J. M. Himpsl, and H. L. Mobley.** 1999. Isolation of *Helicobacter pylori* genes that modulate urease activity. J. Bacteriol. **181:**2477-2484.

8. **Olson, J. W., N. S. Mehta, and R. J. Maier.** 2001. Requirement of nickel metabolism proteins HypA and HypB for full activity of both hydrogenase and urease in *Helicobacter pylori.* Molec. Microbiol. **39:**176-182.

9. **Paschos, A., R. S. Glass, and A. Böck.** 2001. Carbamoylphosphate requirement for synthesis of the active center of [NiFe]-hydrogenases. FEBS Lett. **488:**9-12.

10. **Pragai, Z., H. Tjalsma, A. Bolhuis, J. M. van Dijl, G. Venema, and S. Bron.** 1997. The signal peptidase II (Isp) gene of *Bacillus subtilis.* Microbiology **143 :**1327-33.

11. **Sambrook, J., E. F. Fritsch, and T. Maniatis.** 1989. Molecular cloning: a laboratory manual, 2nd ed. Cold Spring Harbor Laboratory, Cold Spring Harbor, NY.

12. **Thoden, J. B., G. N. Phillips, Jr., T. M. Neal, F. M. Raushel, and H. M. Holden.** 2001. Molecular structure of dihydroorotase: a paradigm for catalysis through use of a binuclear metal center. Biochemistry **40:**6989-6997.

13. **Weatherburn, M. W.** 1967. Phenol-hypochlorite reaction for determination of ammonia. Anal. Chem. **39:**971-974.

14. **Zhang, J. W., G. Butland, J. F. Greenblatt, A. Emili, and D. B. Zamble.** 2005. A role for SlyD in the *Escherichia coli* hydrogenase biosynthetic pathway. J. Biol. Chem. **280:** 4360-4366.

CHAPTER 4

Functional Fusion of the UreE and UreF Urease Accessory Proteins in *Klebsiella aerogenes*

These studies will be published in J. Bacteriol. (2006)

ABSTRACT

Urease is a nickel-containing enzyme that typically requires four accessory proteins (UreD, UreE, UreF, and UreG) for proper incorporation of the metals into the active site. Among these accessory proteins, UreD and UreF have been elusive targets for biochemical and structural characterization because they cannot be overproduced as soluble proteins. In the best-studied system from *Klebsiella aerogenes*, the UreEF fusion protein was generated by a translational fusion of *ureE* and *ureF*. The UreEF fusion protein was overproduced in *Escherichia coli* as a soluble protein with a convenient tag involving the His-rich region of UreE. The fusion protein was functional on the basis of its ability to form a UreD(EF)G-urease apoprotein complex and activate urease *in vivo*, and based on its *in vitro* interaction with UreD-urease apoprotein to form a UreD(EF)-urease apoprotein complex. While the UreF portion of UreEF is fully capable, the fusion significantly affected the role of the UreE portion by interrupting its dimerization and altering its metal binding properties compared to the wild-type UreE. Analysis of a series of UreEF deletion mutants revealed that the C-terminus of UreF is required to form the UreD(EF)G-urease apoprotein complex while the N-terminus of UreF is essential for activation of urease.

INTRODUCTION

Urease is a nickel-containing enzyme that catalyzes the hydrolysis of urea in plants, selected fungi, and many bacteria (1). The bacterial enzyme is especially well studied because it functions as a virulence factor and is implicated in urinary stone formation and gastric ulceration (2).Crystallographic analyses reveal that the three structural subunits (encoded by *ureA*, *ureB*, and *ureC*) of most bacterial ureases associate into a trimer of trimers $[(\alpha\beta\gamma)_3]$, with each UreC subunit containing a dinuclear nickel active site bridged by a carbamylated lysine (3-5). Variations on this theme are found in strains of *Helicobacter*, where the two shorter structural genes are fused and the resulting gene products assemble into a larger macromolecular complex $[((\alpha\beta)_3)_4]$ (6), and in fungi and plants where all three genes are fused to yield a single gene product that associates into a homotrimeric or homohexameric enzyme (7). The nickel ions are essential for the urease catalytic mechanism and function to bind and activate both substrate and the hydrolytic water molecule (1,8).

In addition to the extensive literature related to the enzyme itself, much effort has focused on the steps of urease metallocenter assembly (9). This multi-step process is guided by the action of several accessory proteins that, in bacteria, are typically encoded by genes located in the same cluster as the structural genes. *Klebsiella aerogenes* possesses the best-studied urease activation system involving the *ureDABCEFG* urease gene cluster, where UreD, UreF and UreG form a GTP-dependent molecular chaperone (10) and UreE

functions as a metallochaperone by delivering nickel to the assembled active site (11-13). Among these accessory proteins, only UreE and UreG are highly soluble, resulting in the publication of many studies to characterize these proteins (primarily from *K. aerogenes* and *Bacillus pasteurii*) at a biochemical and structural level (11,14-18). Unlike UreE and UreG, very little is known about UreD and UreF as individual proteins because they are insoluble when overexpressed in *Escherichia coli*. As an attempt to obtain a soluble form of UreF, the *K. aerogenes* homologue was produced as a fusion protein with the maltose-binding protein in *E. coli*; however, no further characterization of the fusion protein was described and, when separated from the maltose-binding domain by digestion with Factor Xa, the UreF protein was unstable (19).

Sequence analysis of the urease gene cluster in *Bordetella bronchiseptica*, a common ureolytic pathogen, revealed that *ureE* and *ureF* are fused to form a single gene in this organism (20). That study suggested the intriguing idea that the UreEF fusion protein may result in tighter coordination of the functions of the two proteins, ensuring productive incorporation of nickel by preventing premature nickel binding before the correct formation of the active site. I hypothesized that the fusion of *K. aerogenes ureE* and *ureF* genes may encode a functional protein and the highly soluble nature of UreE may assist in rendering UreF more soluble as a fusion protein.

Here, I demonstrate that a translational fusion of *K. aerogenes ureE* to *ureF* forms a soluble UreEF fusion protein with a convenient purification tag involving the His-rich sequence of UreE (ten His in the C-terminal 15 residues). I

show that the UreEF fusion protein is functional based on its interactions with other urease components and its participation in urease activation. I exploit properties of this fusion to determine that interactions with other urease components require the C-terminus of UreF and that the N-terminus of UreF is essential for urease activation. I also provide a biochemical characterization of the purified UreEF fusion protein.

MATERIALS AND METHODS

Plasmid Construction—All restriction digestions and DNA manipulations were performed by following standard procedures (21). Primers were synthesized at Integrated DNA Technologies, Inc. (Coralville, Iowa) for construction of plasmids used in this study (Table 1). Site-directed mutagenesis was performed to introduce two nucleotides (GC) before the stop codon of *ureE*, using pTBEF (22) as a template and the QuickChange mutagenesis kit (Stratagene). This procedure removed the stop codon of *ureE* by frame shift, created a new *Nhe*I site for easy screening of the mutant plasmid, and inserted two extra amino acids (Ala Ser) between UreE and UreF. The resulting plasmid (pTBEF-GCins), containing a translational fusion of the *ureE* and *ureF* genes, was digested with *Bst*XI and *Aat*II, and cloned into similarly digested pKK17 (16) to yield pKK-EF. pKK-ΔE and pKK-ΔF were generated by the subcloning procedures described in Table 1, using pACT-KKΔ2-136f (13) and pKAU17Δ*ureF*

Table 1. Plasmids and Primers used

Plasmid or primer	Description	Reference
Plasmids		
pKAU17	*K. aerogenes ureDABCEFG* genes cloned into pUC8	(41)
pTBEF	*Bam*HI-*Avr*II fragment of pKAU17 (containing *ureEF*) cloned into *Bam*HI/*Xba*I-digested pUC19	(22)
pTBEF-GCins	pTBEF with a translational fusion of *ureE* and *ureF* genes by introducing two nucleotides (GC) before the stop codon of *ureE*; creating a new *Nhe*I site and encoding two extra amino acids (Ala Ser)	This study
pKK17	*K. aerogenes ureDABCEFG* genes on an *Eco*RI-*Hin*dIII fragment cloned into pKK223-3	(16)
pKK-EF	*Bst*XI-*Aat*II fragment of pTBEF-GCins cloned into similarly digested pKK17	This study
pACT-KKΔ2-136f	pACT3 containing *ureDABCEFG* with a deletion of *ureE* residues 2 to136	(13)
pKK-ΔE	*Bst*XI-*Aat*II fragment of pACT-KKΔ2-136f cloned into similarly digested pKK17	This study
pKAU17Δ*ureF* L2	pKAU17 with *ureF* deletion by removal of *Aat*II-*Avr*II fragment of pKAU17	(23)
pKK-ΔF	*Bst*XI-*Kpn*I fragment of pKAU17Δ*ureF* L2 cloned into similarly digested pKK17	This study
pETH144* ΔG	pET21 containing *ureEF* with a deletion of the His-rich C terminus of UreE	(16)
pET-EF	*Bam*HI-*Aat*II fragment of pTBEF-GCins cloned into similarly digested pETH144* ΔG	This study
pK-EFG	*Bam*HI-*Kpn*I fragment (containing *ureEF* fusion and *ureG*) of pKK-EF cloned into similarly digested pUC19	This study
NΔ24	Same as pKK-EF but with a truncated *ureEF* gene lacking the N-terminal 24 residues of UreF	This study
CΔ15	Same as pKK-EF but with a truncated *ureEF* gene lacking the C-terminal 15 residues of UreF	This study
CΔ49	Same as pKK-EF but with a truncated *ureEF* gene lacking the C-terminal 49 residues of UreF	This study
Primers		
NΔ24 For	5'-TGGTCCCAGGGGCTGGAGTGGGCTGTG-3'	
NΔ Rev	5'-GCTAGCGTGGCTGTGAGCGTGGTGGTC-3'	
CΔ15 Rev	5'-GATGGCGGCGAGCGGGGTGGCCGATCC-3'	
CΔ49 Rev	5'-CTGGGCGGCCTGCTGGCCGAAGGG-3'	
CΔFor	5'-TAGGAGAAGCCATGAACTCTTATAAACACCCGCTGC-3'	

L2 (23), respectively. pET-EF was constructed by cloning the *Bam*HI-*Aat*II fragment of pTBEF-GCins into similarly digested pETH144*ΔG, resulting in the insertion of the *ureEF* fusion gene into pET21 for purification of the fusion protein. To construct a template plasmid for generation of deletion mutants of the UreEF fusion protein, pKK-EF was digested with *Bam*HI and *Kpn*I, and the resulting fragment (covering the *ureEF* fusion gene and *ureG*) was cloned into pUC19 to yield pK-EFG. Mutants with deletions at either the N or C terminus of UreF in the UreEF fusion protein were obtained by PCR-based methods by using the primers indicated (Table 1) and *pfu* Turbo DNA polymerase (Stratagene). After sequencing, each deletion mutant plasmid was digested with *Bst*XI and *Kpn*I, and the appropriate fragment was subcloned into similarly digested pKK-EF to replace the *ureEF* fusion fragment.

Bacterial Strains and Culture Conditions—*E. coli* C41(DE3) cells (24) were used as host for expression for all plasmids. *E. coli* transformants were cultured in Terrific Broth (TB, Fisher Biotech) supplemented with appropriate antibiotics at 37 °C to an OD_{600} ~ 0.4, induced with 0.5 mM isopropyl β-D-thiogalactopyranoside (IPTG[1], Roche), and harvested after 14-16 hr. Cultures for urease activity measurements were grown with supplementary $NiCl_2$ in the medium under the same conditions described above.

Preparation of Cell Extracts for Urease and Protein Assays—Cell pellets were resuspended in 20 mM Tris buffer (pH 7.4) containing 150 mM NaCl

and 1 mM EDTA (STE buffer), and disrupted by sonication (Branson Sonifier). Intact cells and debris were removed by centrifugation at 10,000 *g* for 20 min at 4 °C.

Purification of UreEF Fusion Protein and UreEF-Containing Urease Apoprotein Complexes—UreEF fusion protein and UreEF-containing protein complexes were purified by using the methods described previously (22). Cell pellets of *E. coli* C41 (DE3) containing pET-EF (for UreEF fusion protein) or pKK-EF (for UreEF-containing urease apoprotein complexes) were resuspended in buffer A (20 mM Tris (pH 7.8), 500 mM NaCl, 60 mM imidazole) and disrupted by sonication. The cell extracts were obtained by centrifugation at 100,000 *g* for 45 min at 4 °C, and loaded onto a Ni-nitrilotriacetic acid (NTA) (Novagen) column charged with 50 mM $NiCl_2$ and equilibrated with buffer A. The Ni-NTA resin was washed with buffer A until the A_{280} reached the baseline. Bound proteins were eluted in 20 mM Tris buffer (pH 7.8) containing 500 mM NaCl and 1 M imidazole, and fractions were analyzed by gel electrophoresis. Samples of interest were dialyzed against 20 mM Tris buffer (pH 7.8) containing 85 mM NaCl, 1 mM EDTA, and 20 % glycerol. For equilibrium dialysis and UV-visible spectroscopy, the samples were further dialyzed against the identical buffer without EDTA several times to remove EDTA from the samples.

Ni-NTA pull-down assay—Cell pellets of *E. coli* C41 (DE3)[pET-EF] were resuspended in binding buffer (20 mM Tris (pH7.8), 300 mM NaCl, 60 mM

imidazole), and disrupted by sonication. The resulting cell extracts were incubated for 15 min at room temperature with 200 µl of Ni-NTA slurry (50 % suspension) equilibrated with the binding buffer. The UreEF-bound resin was washed with 10 bed volumes of the binding buffer twice, and incubated with 600 µg *K. aerogenes* UreD-urease apoprotein complex (purified by Soledad Quiroz according to (25)) in 1 mL either for 20 min at room temperature or overnight at 4 °C. After incubation, the resin was washed in the same manner as the first wash, followed by elution with 20 mM Tris (pH 7.8) containing 300 mM NaCl and 1 M imidazole. Eluted proteins were analyzed by polyacrylamide gel electrophoresis.

Polyacrylamide Gel Electrophoresis and Western Blot Analysis—Sodium dodecyl sulfate (SDS)-polyacrylamide gel electrophoresis (PAGE) was carried out for protein analysis with the buffers described by Laemmli (26), and utilized 15%, 13.5%, or 12% polyacrylamide running gels with 4.5% stacking gels. The gels were either stained with Coomassie brilliant blue (Sigma) or electroblotted onto Immobilon-P polyvinylidene difluoride (PVDF) membrane (Millipore), probed with anti-*K. aerogenes* UreE antibodies (27) or anti-*K. aerogenes* UreG antibodies (17), and visualized with anti-rabbit immunoglobulin G-alkaline phosphatase conjugates (Sigma).

Urease and Protein Assays—Urease activity was measured by quantifying the rate of ammonia release from the hydrolysis of urea by formation of indophenol, which was monitored at 625 nm (28). One unit of urease activity

(U) was defined as the amount of enzyme required to hydrolyze 1 μmol of urea per min at 37 °C. The standard assay buffer contained 50 mM HEPES (*N*-2-hydroxyethylpiperazine-*N'*-ethanesulfonic acid; pH 7.8) and 50 mM urea. Protein concentrations were determined by using a commercial assay (Bio-Rad) with bovine serum albumin as the standard (29).

Gel Filtration Chromatography—The native molecular weight of the purified UreEF fusion protein was estimated by gel filtration chromatography using two different columns, a KW-804 (8 x 300 mm, Shodex) and a Protein-Pak 125 column (7.8 x 300 mm, Waters), connected to a Waters Breeze chromatography system. Isocratic elution utilized 20 mM Tris buffer (pH 7.8) containing 200 mM NaCl and 0.1 mM EDTA. Mixtures of protein molecular weight standards (Bio-Rad) were used to standardize the columns.

Equilibrium Dialysis—Protein samples (10 μM in 50 mM Tris buffer (pH 7.8) containing 85 mM NaCl) were dialyzed against the identical buffer containing varied concentrations of $^{63}NiCl_2$ (1,445 mCi/mmol; Du Pont NEN Research Products, Inc., Wilmington, DE), using an equilibrium microvolume dialyzer (Hoefer Scientific Products, San Francisco, CA) equipped with dialysis membranes (MW cutoff 10,000, Spectra/Por). After overnight equilibration at 4 °C, an aliquot from each compartment was measured for radioactivity by using a Beckman LS7000 liquid scintillation system and Bio-Safe II scintillation fluid

(Research Products International Corp.). Data were fitted to a two-cooperative-site Adair equation, as described previously (16).

UV-Visible Spectroscopy—Electronic absorption spectra of wild-type UreE (100 μM monomer) and UreEF fusion proteins (47 μM monomer) in the presence of increasing concentrations of varied divalent metal ions were analyzed on a Shimadzu 2401PC spectrophotometer with a 1 ml cuvette in 50 mM Tris buffer (pH 7.8) containing 85 mM NaCl.

RESULTS

Expression of Recombinant *K. aerogenes* UreEF Fusion Protein in *E. coli*—To generate the *K. aerogenes* UreEF fusion protein and determine whether the fusion protein is functional in terms of urease activation, the *ureE* and *ureF* genes were translationally fused by adding two nucleotides (GC) before the stop codon of *ureE* in pKK17 (containing the entire *K. aerogenes* urease operon, see Table 1). This mutation eliminated the stop codon of *ureE* by frame shift and inserted two extra amino acids (Ala Ser) between UreE and UreF, as illustrated in Fig. 1A. The resulting plasmid pKK-EF was transformed into *E. coli* C41 (DE3) cells for overexpression. The cell extracts of cultures containing pKK-EF did not contain the UreE band like that detected in cell extracts of *E. coli* C41 (DE3)[pKK17], but they possessed a new protein band with an apparent

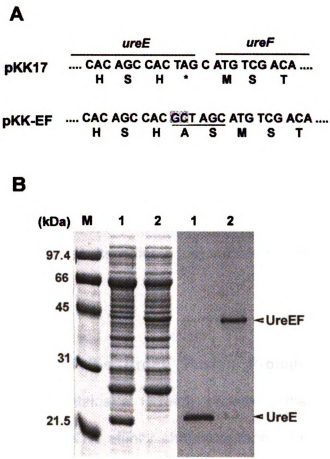

Figure 1. Expression of the *K. aerogenes ureEF* fusion gene in *E. coli*. (A) Nucleotide sequence of the junction of the translationally fused *ureE* and *ureF* genes in pKK-EF. Addition of the two nucleotides (GC) before the stop codon of *ureE* is shown in a shaded box. This creates an *Nhe*I site indicated by underline, encoding the two extra amino acids (Ala Ser). (B) (Left panel) cultures carrying pKK17 or pKK-EF were induced with 0.5 mM IPTG. The cell extracts were analyzed by sodium dodecyl sulfate-polyacrylamide gel electrophoresis, and visualized by Coomassie Blue staining. Lanes: M, molecular weight markers; 1, cell extracts of *E. coli* C41 (DE3)[pKK17]; 2, cell extracts of *E. coli* C41 (DE3)[pKK-EF]. (Right panel) Western blot with anti-UreE antibodies for samples described in lanes of the left panel.

molecular weight of ~ 43 kDa that was the size expected for the product arising from the fusion of *ureE* and *ureF* genes (Fig. 1B, left). To confirm that the new protein band is the UreEF fusion protein, a Western blot analysis with anti-UreE antibody was performed. A single immunoreactive band was detected in *E. coli* C41 (DE3)[pKK-EF] cell extracts, which is at the same position as the band visualized by Coomassie Blue staining (Fig. 1B, right). As expected, *E. coli* C41 (DE3)[pKK17] cell extracts had a single immunoreactive band running at the position of UreE. These results indicate that soluble *K. aerogenes* UreEF protein can be produced in *E. coli*.

Copurification of the UreEF Fusion Protein with Other Urease Components—UreE contains a His-rich sequence that allows for one-step purification by using Ni-NTA affinity chromatography. In addition to facilitating purification, this chromatography approach may be employed for detecting protein-protein interactions by examining the proteins that copurify with the target protein. To explore the possible protein-protein interactions that occur among urease components (both structural and accessory proteins) *in vivo*, cell extracts of *E. coli* C41 (DE3) cultures containing pKK17 or pKK-EF were subjected to Ni-NTA column chromatography. As shown in Fig. 2, purified protein from *E. coli* C41 (DE3)[pKK17] cell extracts was exclusively UreE, indicating that UreE did not exhibit stable interactions with other urease components. In contrast, when starting with *E. coli* C41 (DE3)[pKK-EF] the UreEF fusion protein copurified with the urease structural proteins (UreABC), two other urease accessory proteins

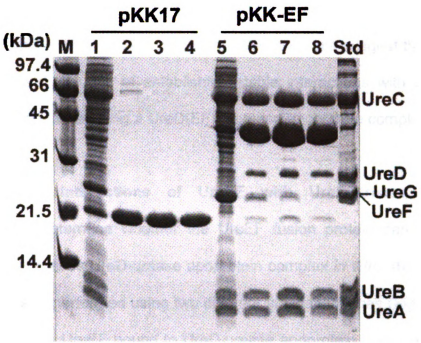

Figure 2. Co-purification of other urease components with the UreEF fusion protein. *E. coli* C41 (DE3) cultures harboring pKK17 or pKK-EF were induced with 0.5 mM IPTG, and the cell extracts were subjected to Ni-NTA column chromatography. Eluted fractions of the purified proteins were analyzed by SDS-PAGE. Lanes: M, molecular weight markers; 1, cell extracts of *E. coli* C41 (DE3)[pKK17]; 2-4, fractions 2-4 of eluted proteins from these extracts; 5, cell extracts of *E. coli* C41 (DE3)[pKK-EF]; 6-8, fractions 2-4 of eluted proteins from these extracts; Std, purified *K. aerogenes* UreDFG-urease apoprotein complex.

(UreD and UreG), and an unknown protein with a molecular weight of ~ 20 kDa. This unknown protein band ran at a similar position to UreE on the gel, but it was not a degradation product of the UreEF based on the lack of immunoreactivity using anti-UreE antibody (data not shown). These results suggest that the UreEF fusion protein is capable of establishing stable interactions with other urease components *in vivo*, forming a UreD(EF)G-urease apoprotein complex.

***In vitro* Interactions of UreEF with UreD-Urease Apoprotein Complex**—To determine whether the UreEF fusion protein can interact with purified *K. aerogenes* UreD-urease apoprotein complex *in vitro*, the Ni-NTA pull-down assay was performed using two different incubation times (Fig. 3). For both conditions tested, UreEF bound to UreD-urease apoprotein complex *in vitro*, but at sub-stoichiometric levels of the complex that did not equate to the input amount. The observed low stoichiometry suggests that additional cellular components such as molecular chaperones might facilitate the interaction of these proteins within the cell. The binding of UreEF to UreD-urease apoprotein complex was highly specific as shown by the lack of interaction with contaminant proteins present in the purified UreD-urease apoprotein complex (lane 2).

Effects of the UreEF Fusion on Urease Activity—The observation that the UreEF fusion protein interacts with other urease components indicated that the fusion protein might be functional in urease activation. To assess the effects of the fusion on individual functions of UreE and UreF, urease activities were

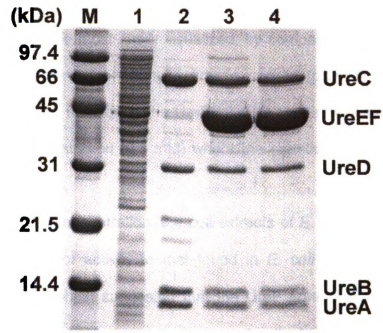

Figure 3. *In vitro* interactions of UreEF with UreD-urease apoprotein complex. Cell extracts of *E. coli* C41 (DE3)[pET-EF] were incubated with Ni-NTA resin, and the UreEF-bound resin was incubated with purified UreD-urease apoprotein complex at two different conditions. Eluted protein complexes were analyzed by SDS-PAGE. Lanes: M, molecular weight markers; 1, cell extracts of *E. coli* C41 (DE3)[pET-EF]; 2, purified *K. aerogenes* UreD-urease apoprotein complex; 3, eluted proteins after incubation of UreEF-bound Ni-NTA resin with UreD-urease apoprotein complex for 20 min at room temperature; 4, eluted proteins after incubation of the mixture overnight at 4 °C

measured in cell extracts of *E. coli* C41(DE3) containing pKK17 or pKK-EF and grown under high or limiting nickel conditions. The effect of the fusion on the function of UreF was examined at high nickel concentration (5 mM), where the effect was likely to be most easily visualized, by comparing to the activity levels found in cells carrying the wild-type urease operon (pKK17). In contrast, the assessment of UreE function in the UreEF fusion protein was examined using a limiting nickel concentration (0.5 mM) where the metallochaperone role is more pronounced.

At a high nickel concentration, the cell extracts of *E. coli* C41 (DE3)[pKK-EF] had a similar level of activity to that found in *E. coli* C41 (DE3)[pKK17] cell extracts (Fig. 4A), which suggested that the UreF portion of the UreEF fusion protein is fully functional, in good agreement with its ability to form a stable complex with other urease components (Figs. 2 and 3). Deletion of the *ureE* gene from the urease operon (creating plasmid pKK-ΔE) decreased the activity by ~ 40 %, compared to *E. coli* C41 (DE3)[pKK17]. As expected, very low activity was observed in the case of deletion of the *ureF* gene from the cluster (generating plasmid pKK-ΔF), which is consistent with our previous studies showing that UreF is essential for urease activation (23). At limiting nickel conditions, however, a significant decrease in urease activity was observed in extracts of *E. coli* C41 (DE3)[pKK-EF] compared to that found in control cell extracts. In fact, the level of activities was comparable to that detected in extracts of *E. coli* C41 (DE3)[pKK-ΔE], which indicated that the function of UreE in the UreEF fusion protein was greatly compromised by the fusion (Fig. 4B).

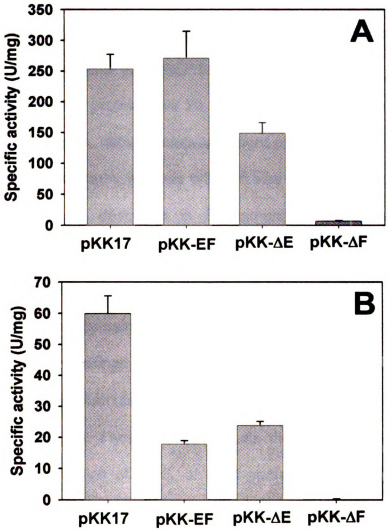

Figure 4. Urease activity in recombinant *E. coli* C41 (DE3) cell extracts containing the indicated plasmids. The cells were grown with 5 mM Ni^{2+} (A) or 0.5 mM Ni^{2+} (B) in TB medium. Error bars represent the standard deviation for three separate determinations.

Characterization of the Purified Recombinant *K. aerogenes* UreEF Fusion Protein—Recombinant *K. aerogenes* UreEF fusion protein was purified by Ni-NTA affinity chromatography from *E. coli* C41 (DE3) cells containing pET-EF, which includes only the *ureEF* fusion gene in the pET21 expression vector. Typical yields of the protein were 20-30 mg per liter of culture. Using the purified UreEF fusion protein, native molecular weight estimations were performed by gel filtration chromatography with two different size exclusion columns, KW-804 and ProteinPak-125, as described in Experimental Procedures. Data from the chromatographic analysis with KW-804 allowed estimation of the native size of the UreEF fusion protein to be 43.0 ± 1.6 kDa, consistent with a monomeric structure. Analysis by using ProteinPak-125 column gave similar results (51.7 ± 0.9 kDa). These findings support the notion that the UreEF fusion protein is monomeric, rather than the dimer that was anticipated by the dimeric structure of wild-type UreE (14). These results indicate that the fusion of UreE and UreF prevented dimerization of UreE, at least partially accounting for the perturbed UreE function of the UreEF fusion protein (Fig. 4B).

The monomeric structure of the UreEF fusion protein led us to examine the metal binding properties of the UreEF fusion protein and compare to those of wild-type UreE protein. The number of nickel ions that bound to the UreEF fusion protein was determined for a range of nickel concentrations by equilibrium dialysis, and the data were fitted to a two-cooperative-site Adair equation (16). The UreEF fusion protein binds 3.32 ± 0.17 mol of nickel per mole of monomer with a K_{d1} of 64.0 ± 10.4 μM and a K_{d2} of 7.0 ± 2.1 μM, which compares to about

6 nickel ions per wild-type UreE homodimer with an average K_d of 9.6 μM (27). The metal binding properties of the UreEF fusion protein were further characterized by UV-visible spectroscopy and compared to the spectra of metal-bound wild-type UreE. Many studies have focused on spectroscopic metal binding analysis of H144* UreE that lacks the His-rich carboxyl terminus (11,13,22,30), but no UV-visible studies have been reported on wild-type UreE until this analysis. As illustrated in Fig. 5, the UreEF fusion protein exhibited distinct UV-visible spectra from those of wild-type UreE for all three metal ions. Binding of Cu^{2+} to wild type UreE resulted in a significant increase in absorbance at 366 nm, caused by a thiolate-to-Cu^{2+} charge-transfer transition involving Cys79 (30), while this feature is completely absent in the corresponding spectrum of the UreEF fusion protein (Fig. 5A and 5B). A plot of the absorbance changes at 366 nm versus the Cu^{2+} concentration exhibited sigmoidal effects for wild-type UreE, with a midpoint Cu^{2+} concentration of 2.60 ± 0.04 mol of Cu^{2+}/ mole of monomer (inset in Fig. 5A). In contrast, only a broad feature near 700 nm along with a uniform increase throughout the spectrum was generated when cupric ions were added to the fusion protein. There was no turbidity detected in this sample throughout the titration ruling out protein aggregation. The addition of Ni induced an absorbance increase at 366 nm as well as an increase throughout the spectrum in wild-type UreE, but neither of these features is as pronounced in the UreEF fusion protein (Fig. 5C and 5D). Similar differences were noted when Co^{2+} was added to the two proteins. The lack of thiolate-to-metal charge transfer

Figure 5. UV-visible spectra of wild type UreE and the UreEF fusion protein titrated with selected metal ions. (A, C, E) Raw data from titration of 100 μM UreE with divalent Cu, Ni, and Co in 20 mM Tris buffer (pH 7.8) containing 85 mM NaCl and 20 % glycerol, respectively. Inset in (A) shows data from the same titration of UreE with Cu shown in (A) and corrected for dilution effects to calculate the extinction coefficient at 366 nm. (B, D, F) Raw data from titration of 47 μM UreEF fusion protein with Cu, Ni, and Co in the identical buffer conditions, respectively.

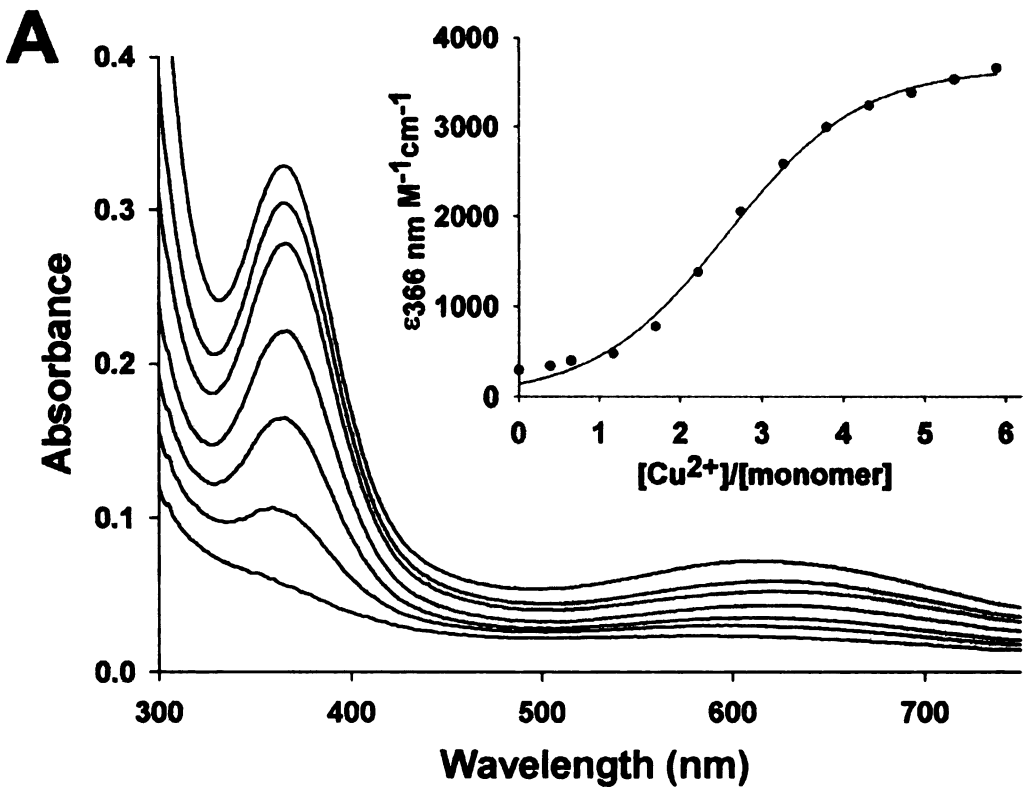
A
Absorbance
0.4
0.3
0.2
0.1
0.0
300
400
500
600
700
Wavelength (nm)
ε366 nm M-1cm-1
4000
3000
2000
1000
0
0
1
2
3
4
5
6
[Cu2+]/[monomer]

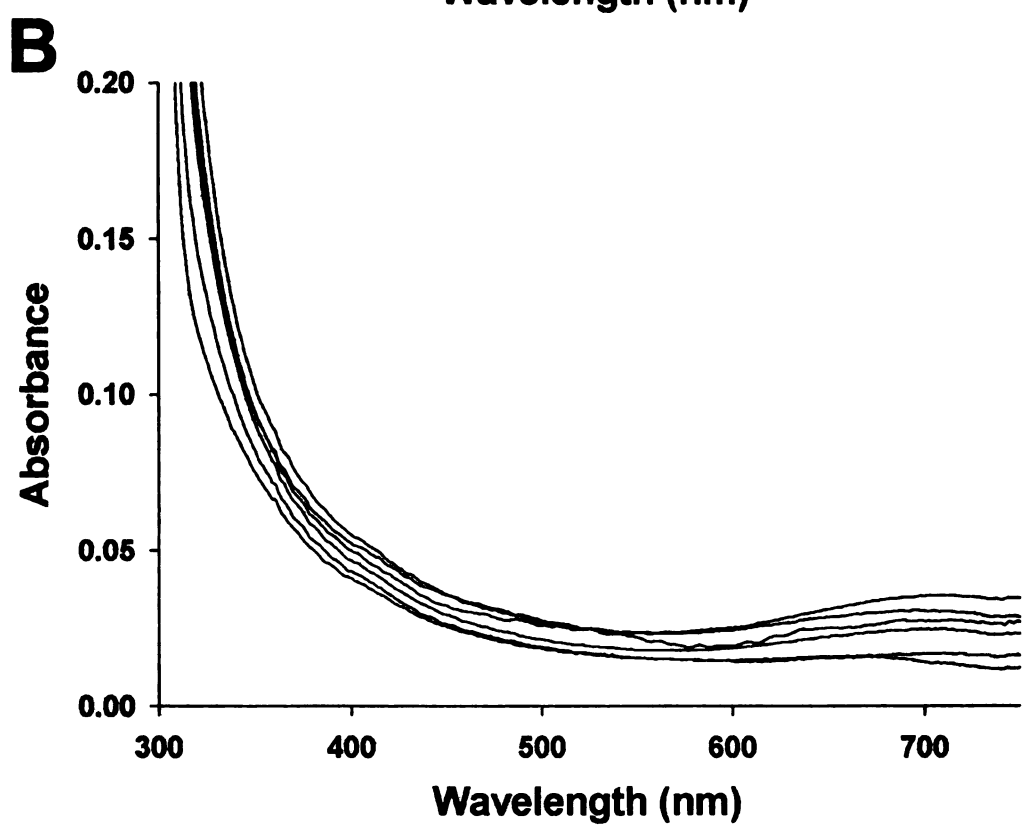
B
Absorbance
0.20
0.15
0.10
0.05
0.00
300
400
500
600
700
Wavelength (nm)

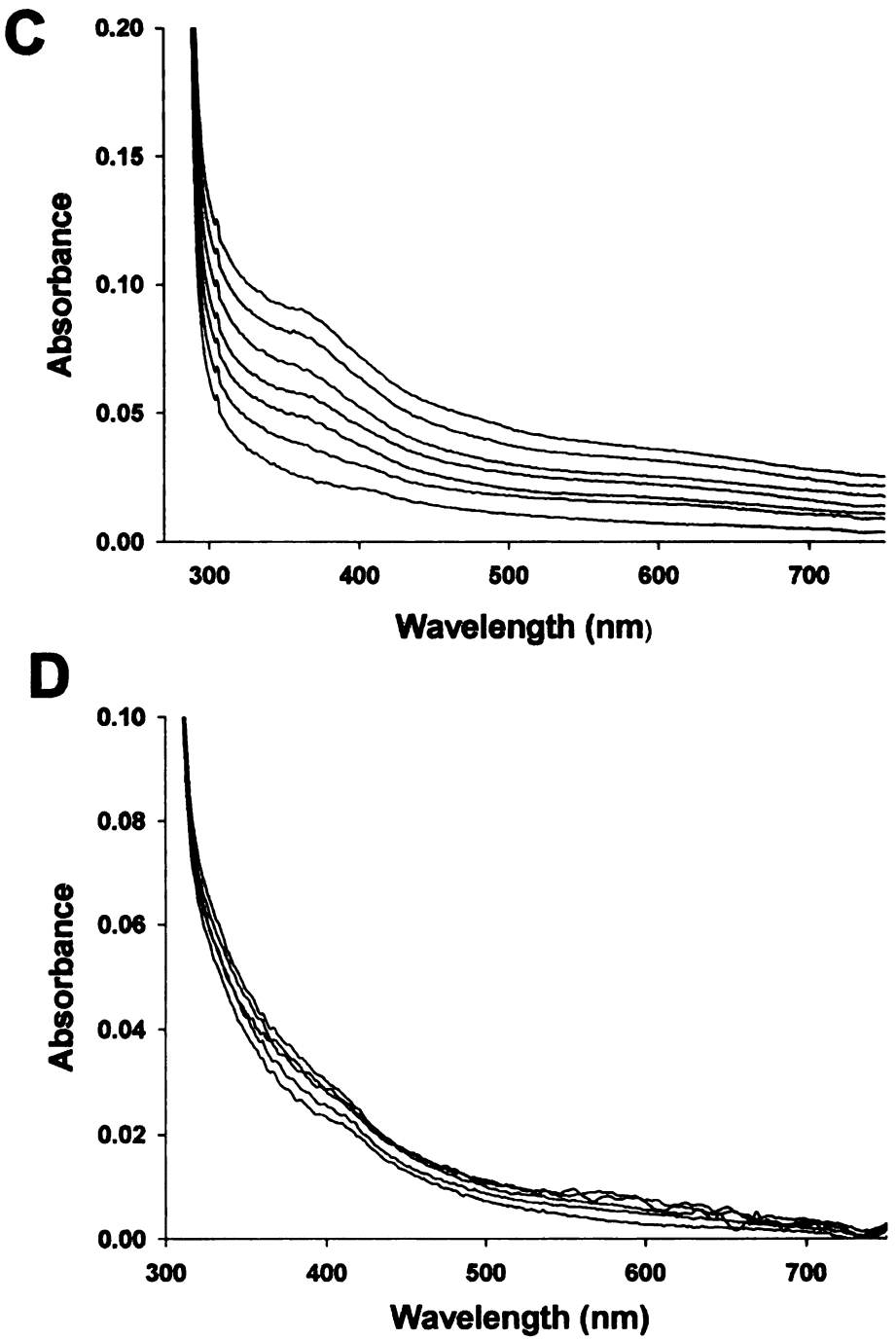

Figure 5. (cont'd).

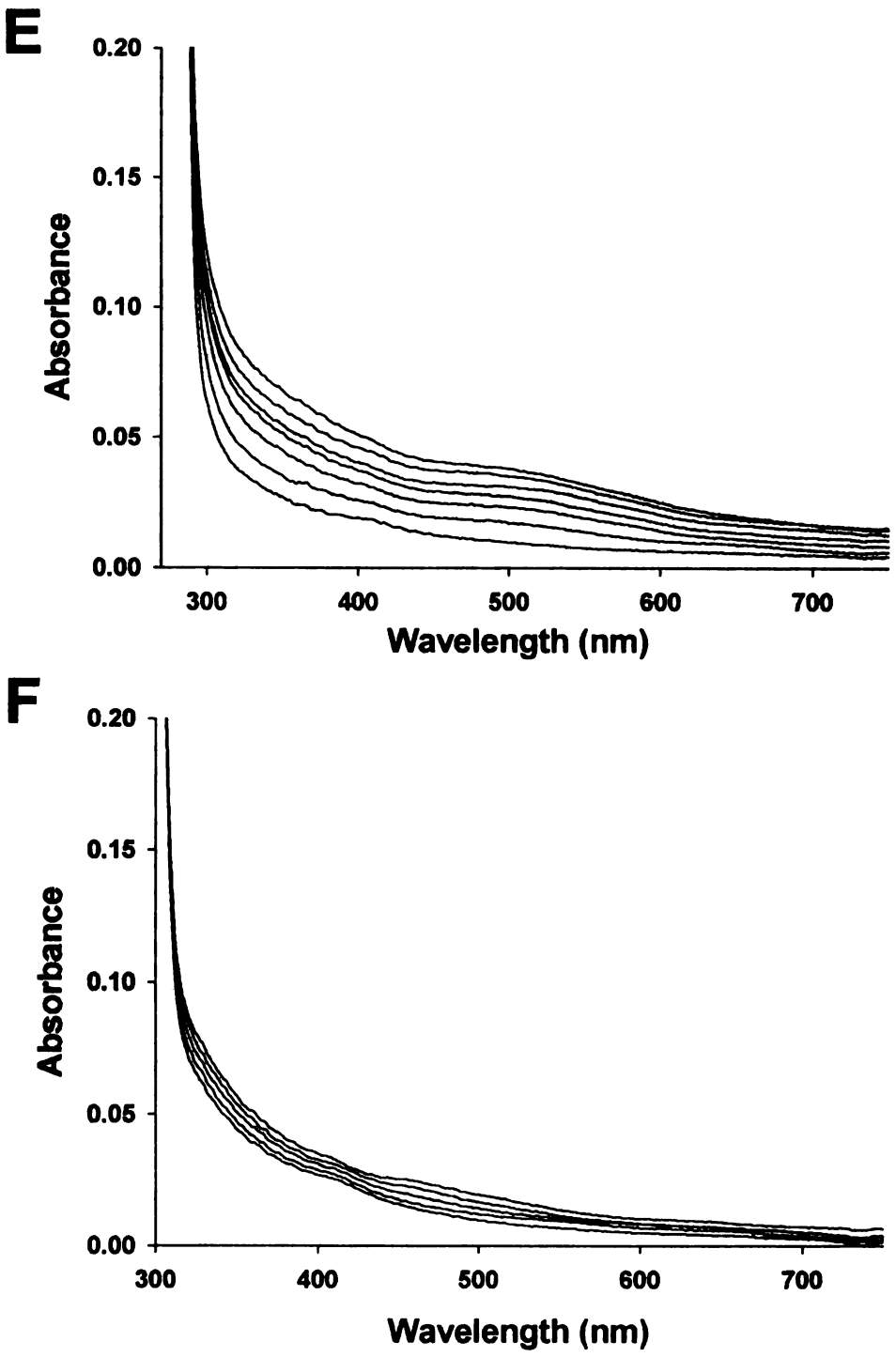

Figure 5. (cont'd).

transitions suggest that, unlike the case for wild-type UreE, the Cys79 of the UreEF fusion protein is not accessible for metal binding in solution.

Effects of UreEF Deletions on Interactions With Other Urease Components and Function as a Molecular Chaperone—To gain further insight into the interactions of UreEF fusion protein with other urease components (Fig. 2) in relation to its function, N- or C- terminal deletion mutants of UreEF were generated by in-frame truncation of amino acid residues of UreF, as illustrated in Fig. 6A. As shown in Fig. 6B, deletion of 24 residues at the UreF N-terminus did not affect its interactions with other urease components in the complex. The urease subunits and UreD were clearly visible in this sample while UreG was not distinguishable on the gel because of the lower band intensity and the presence of other non-specific proteins similar in molecular weight to UreG. However, UreG was detected on a Western blot with anti-UreG antibodies using the same sample, suggesting that UreG is less stably associated with the urease apoprotein complex than UreD and UreEF (data not shown). Compared to the case of the UreEF control, much lower levels of NΔ24 mutant protein were purified due to its decreased solubility caused by the truncation. However, this protein level roughly correlated to a stoichiometric ratio with other urease components (UreABC and D), indicating that the deletion mutant protein is primarily in the complex (UreD(NΔ24/EF)-urease apoprotein), rather than a mixture of free protein and protein in the complex as observed in the case of UreEF control.

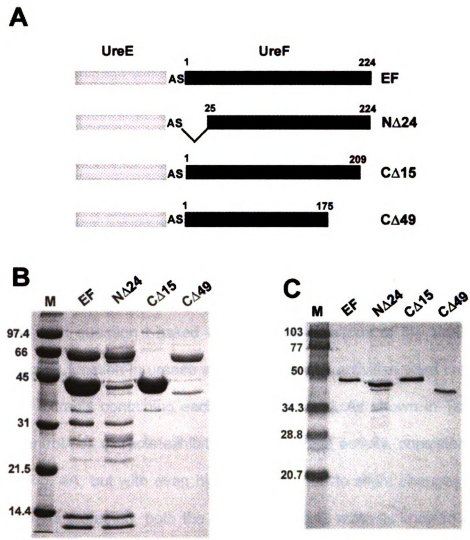

Figure 6. Interactions of the UreEF deletion mutants with other urease components. (A) Schematic diagram of the N- or C-terminal deletion mutants of the UreEF fusion protein. Deletions are denoted by the black rectangles starting and ending at the designated amino acid sequence number of UreF. The linker sequence generated by the fusion of UreE and UreF is indicated by AS (Ala Ser). (B) Interactions of UreEF deletion mutants with other urease components. *E. coli* cultures expressing the entire urease gene cluster containing each UreEF deletion mutant were used for monitoring protein-protein interactions, following the same procedures as described in Figure 2. (C) Expression of UreEF deletion mutants. Deletion mutant proteins in cell extracts were visualized by Western blot analysis with anti-UreE antibodies.

As opposed to the N-terminal deletion, truncation of the C-terminus of UreF totally abolished the interactions with other urease components in the complex. As in the case with NΔ24, the CΔ49 mutant produced very little soluble protein, which resulted in much smaller protein levels after Ni-NTA column purification, and a major non-specific band (~ 60 kDa) was more prominent (Fig. 6B). I also generated the CΔ61 mutant but encountered a similar problem, indicating that more truncation caused decreased solubility of the protein (data not shown). Nevertheless, all deletion mutants tested produced some soluble proteins as detected by Western blot analysis with anti-UreE antibodies (Fig. 6C).

The next question I asked was how the deletions of the UreEF protein would affect its function in urease activation. Urease activities were measured in *E. coli* cell extracts containing each deletion mutant. As shown in Table 2, the pKK-EF control cell extracts exhibited a high urease activity, consistent with the results in Fig. 4A, but with even higher activity due to slight changes in culture conditions. As expected, both the CΔ15 and CΔ49 mutants showed almost no activities, in good agreement with their inability to interact with other urease components in the complex. Surprisingly, the NΔ24 mutant also failed to activate urease and conferred low activity comparable to the C-terminal deletion mutants of UreEF. These results suggest that the N-terminus of UreF is not required for protein-protein interactions in the complex, but it is essential for UreF to function as a molecular chaperone in the process of urease activation.

Table 2. Urease activity in recombinant *E. coli* C41 (DE3) cell extracts containing the indicated UreEF deletion mutants grown with 5 mM $NiCl_2$

Cultures	Specific activity [a] (μmol of urea /min /mg)
pKK-EF	384 ± 30
NΔ24	0.141 ± 0.018
CΔ15	0.296 ± 0.086
CΔ49	0.19 ± 0.14

[a]Values are the averages of three separate determinations ± standard deviation.

DISCUSSION

Urease is one of many metalloenzymes that require accessory proteins for the production of catalytic activity (31). *K. aerogenes* possesses the best-characterized urease metallocenter assembly system, and utilizes four accessory proteins (UreD, UreE, UreF, and UreG). Many studies have focused on the steps of urease metallocenter assembly by examining the various multi-protein complexes, composed of apoenzyme and accessory proteins, for their activation properties (32-34). The accessory proteins themselves also have been targets for extensive biochemical and structural studies to gain a better understanding of the process of metallocenter assembly (11,14-18). Among these accessory proteins, UreD and UreF have been elusive subjects for biochemical and structural analyses mainly because the proteins are insoluble when overexpressed in *E. coli*.

I generated the *K. aerogenes* UreEF fusion protein by creating a translational fusion of *ureE* and *ureF* genes. The fusion of UreE to UreF was postulated to have several advantages. First, the high expression levels and solubility of UreE may help to enhance the solubility of UreF as a fusion protein. Secondly, using an adjacent accessory gene in the *ure* operon as a fusion partner would make it easier to examine the function of the fusion protein in urease activation without disrupting the operon structure. Thirdly, the His-rich sequence at the C-terminus of UreE provides a convenient purification tag for the UreEF fusion protein. Of additional interest, the translational fusion of these two

genes had already been reported to occur naturally in another microorganism. Literature precedents have shown that such fusions may be functional, as in a recent study on *Azotobacter vinelandii* nitrogenase where the *nifD* and *nifK* genes were translationally fused to encode a functional MoFe protein that supported nitrogen fixation (35).

The translationally fused UreEF protein is soluble and functional on the basis of its ability to form a UreD(EF)G-urease apoprotein complex and activate urease *in vivo* as well as its capacity to bind UreD-urease apoprotein to form a UreD(EF)-urease apoprotein complex *in vitro*. While the UreF portion of the UreEF fusion protein is fully capable, the fusion significantly affected the role of the UreE portion of the UreEF fusion protein. This could be at least partially explained by the observed properties of the purified UreEF fusion protein. Native molecular weight estimations by gel filtration chromatography revealed that the UreEF protein is monomeric, rather than a dimer that was anticipated by the crystal structure of wild-type UreE. This structural difference is expected to affect the function of the UreE portion of the UreEF protein because the monomeric fusion protein does not possess the critical metal site involving the pair of His96 residues at the interface of wild type UreE dimer and believed to bind Ni that is incorporated into the active site of urease (11,14,16). Nevertheless, the UreEF fusion protein binds ~ 3 mol of nickel per mole of monomer, as determined by the equilibrium dialysis analysis. This metal binding likely involves the His-rich C-terminus of UreE. The C-terminal His-rich sequence was shown to be dispensable for urease activation because the truncated UreE lacking the His-

rich sequence can bind nickel and activate urease (22). Thus, the C-terminal His-rich region of UreE may work as a nickel storage protein, contributing to tight regulation of cellular nickel concentrations. Supporting this hypothesis, the N-terminal His-rich region of HypB protein from *Bradyrhizobium japonicum* was shown to sequester and store nickel for later use in hydrogenase expression and maturation steps during nickel starvation (36,37). It is not yet clear, however, whether the nickel bound to the C-terminal His-rich sequence of UreE can be utilized later for activation of urease or other nickel-dependent enzymes under nickel starvation conditions. UV-visible spectroscopy reveals another aspect of changes in the UreE portion of the UreEF fusion protein. Most notably, Cys79 of UreE is not accessible for metal binding. This seclusion may be caused by physical blocking of the Cys79 residue by UreF, by a conformational change within UreE caused by UreF, or by changes in the pK_a of the sulfhydryl group of Cys79 after the fusion.

Although the fusion of UreE to UreF significantly altered the oligomeric structure and metal binding properties of UreE, it provided a convenient tool to examine the protein-protein interactions between UreEF and other urease components by Ni-NTA affinity chromatography. In particular, I found that UreEF copurified with UreD, UreG, and the UreABC apoprotein, consistent with *in vivo* formation of a UreD(EF)G-urease apoprotein complex. In addition, UreEF binds to UreD-urease apoprotein to form a UreD(EF)-urease apoprotein complex *in vitro*. In contrast, UreEF does not exhibit stable interactions with UreG based on analyses using the Ni-NTA pull-down assay with UreEF and UreG as the only

urease components (data not shown). These results can be compared with previous efforts to examine interactions among the urease components. A yeast two-hybrid analysis of the *H. pylori* system indicated that UreF interacts with UreH (corresponding to UreD in other microorganisms), but not with UreG (38). A similar approach with the *Proteus mirabilis* urease components also revealed that UreF interacts with UreD (39). The yeast two-hybrid results complement our earlier biochemical and immunological findings that the *K. aerogenes* UreD-urease apoprotein complex forms independently of the presence of other accessory proteins (32) and the presence of UreF masks the immunoreactivity of UreD bound to the apoprotein complex (34). In sum, these results suggest that UreD may be crucial for recruitment of the UreF to the apoprotein complexes; i.e., with regard to the present study the UreD tethers UreEF to the UreABC structural subunits. Interactions also may exist directly between UreF and the urease apoprotein. For example, chemical cross-linking / tryptic digestion / mass spectrometry studies showed the existence of a chemical cross-link between the UreF N-terminus (residues 1-7) and UreB Lys76 of the UreDF-urease apoprotein complex (40). It remains unclear how UreG associates with the UreDF-urease apoprotein complex. Although UreG does not tightly bind to the independent UreEF fusion protein, I cannot rule out the possibility of weak or transient UreG-UreEF interactions when the latter protein is present within the UreD(EF)-urease complexes. For example, our comparative mass spectrometric analyses have provided evidence for significant conformational changes between the UreABC apoprotein and UreDF-urease apoprotein complexes (40).

Although I was unable to identify the exact interaction sites among different urease components in the UreD(EF)- and UreD(EF)G-urease apoprotein complexes, the UreEF deletion mutant study provided evidence for distinct sub-domains of UreF with separate functions related to urease activation. I hypothesize that UreF acts in a two-step process where the C-terminus recognizes and binds to the UreD-urease apoprotein, perhaps inducing a conformational change in this complex, thus positioning the N-terminus of UreF in an orientation that can interact with other urease component(s) to achieve urease activation. This scenario fits well with the results from the UreEF deletion mutant study where the NΔ24 mutant (with an intact UreF C-terminus) interacts with the UreD-urease apoprotein complex, but does not lead to its activation, while the C-terminal deletion mutants fail to form any apoprotein complex. This proposal is consistent with all other available data on protein interactions involving UreF described above.

In summary, I demonstrate that the translational fusion of *K. aerogenes ureE* to *ureF* forms a soluble UreEF fusion protein that is useful for further biochemical and structural studies on the UreF protein. UreEF is functional based on its ability to activate urease and its interactions with other urease components; however, the role of the UreE component is somewhat compromised in this fusion. This study also provides new insight into the roles of the N- and C-termini of UreF in protein-protein interactions and urease activation.

REFERENCES

1. Hausinger, R. P., and Karplus, P. A. (2001) in *Handbook of Metalloproteins* (Wieghardt, K., Huber, R., Poulos, T. L., and Messerschmidt, A., eds), pp. 867-879, John Wiley & Sons, Ltd., West Sussex, U.K.

2. Mobley, H. L. T., Island, M. D., and Hausinger, R. P. (1995) *Microbiol. Rev.* **59**, 451-480

3. Jabri, E., Carr, M. B., Hausinger, R. P., and Karplus, P. A. (1995) *Science* **268**, 998-1004

4. Pearson, M. A., Michel, L. O., Hausinger, R. P., and Karplus, P. A. (1997) *Biochemistry* **36**, 8164-8172

5. Benini, S., Rypniewski, W. R., Wilson, K. S., Miletti, S., Ciurli, S., and Mangani, S. (1999) *Structure* **7**, 205-216

6. Ha, N.-C., Oh, S.-T., Sung, J. Y., Cha, K.-A., Lee, M. H., and Oh, B.-H. (2001) *Nature Structure Biology* **8**, 505-509

7. Sheridan, L., Wilmont, C. M., Cromie, K. D., van der Logt, P., and Phillips, S. E. V. (2002) *Acta Crystallogr.* **D58**, 374-376

8. Ciurli, S., Benini, S., Rypniewski, W. R., Wilson, K. S., Miletti, S., and Mangani, S. (1999) *Coord. Chem. Rev.* **190-192**, 331-355

9. Mulrooney, S. B., and Hausinger, R. P. (2003) *FEMS Microbiol. Rev.* **27**, 239-261

10. Soriano, A., and Hausinger, R. P. (1999) *Proc. Natl. Acad. Sci. USA* **96**, 11140-11144

11. Colpas, G. J., and Hausinger, R. P. (2000) *J. Biol. Chem.* **275**, 10731-10737

12. Soriano, A., Colpas, G. J., and Hausinger, R. P. (2000) *Biochemistry* **39**, 12435-12440

13. Mulrooney, S. B., Ward, S. K., and Hausinger, R. P. (2005) *J. Bacteriol.* **187**, 3581-3585

14. Song, H. K., Mulrooney, S. B., Huber, R., and Hausinger, R. P. (2001) *J. Biol. Chem.* **276**, 49359-49364

15. Remaut, H., Safarof, N., Ciurli, S., and Van Beeumen, J. (2001) *J. Biol. Chem.* **276**, 49365-49370

16. Colpas, G. J., Brayman, T. G., Ming, L.-J., and Hausinger, R. P. (1999) *Biochemistry* **38**, 4078-4088

17. Moncrief, M. B. C., and Hausinger, R. P. (1997) *J. Bacteriol.* **179**, 4081-4086

18. Zambelli, B., Stola, M., Musiani, F., De Vriendt, K., Samyn, B., Devreese, B., Van Beeumen, J., Dikiy, A., Bryant, D. A., and Ciurli, S. (2005) *J. Biol. Chem.* **280**, 4684-4695

19. Kim, K. Y., Yang, C. H., and Lee, M. H. (1999) *Arch. Pharm. Res.* **22**, 274-278

20. McMillan, D. J., Mau, M., and Walker, M. J. (1998) *Gene* **208**, 243-251

21. Sambrook, J., Fritsch, E. F., and Maniatis, T. (1989) *Molecular cloning: a laboratory manual*, 2nd Ed., Cold Spring Harbor Laboratory, Cold Spring Harbor, NY

22. Brayman, T. G., and Hausinger, R. P. (1996) *J. Bacteriol.* **178**, 5410-5416

23. Lee, M. H., Mulrooney, S. B., Renner, M. J., Markowicz, Y., and Hausinger, R. P. (1992) *J. Bacteriol.* **174**, 4324-4330

24. Miroux, B., and Walker, J. E. (1996) *J. Mol. Biol.* **260**, 289-298

25. Park, I.-S., and Hausinger, R. P. (1996) *Biochemistry* **35**, 5345-5352

26. Laemmli, U. K. (1970) *Nature (London)* **227**, 680-685

27. Lee, M. H., Pankratz, H. S., Wang, S., Scott, R. A., Finnegan, M. G., Johnson, M. K., Ippolito, J. A., Christianson, D. W., and Hausinger, R. P. (1993) *Prot. Science* **2**, 1042-1052

28. Weatherburn, M. W. (1967) *Anal. Chem.* **39**, 971-974

29. Bradford, M. M. (1976) *Anal. Biochem.* **72**, 248-254

30. Colpas, G. J., Brayman, T. G., McCracken, J., Pressler, M. A., Babcock, G. T., Ming, L.-J., Colangelo, C. M., Scott, R. A., and Hausinger, R. P. (1998) *J. Biol. Inorg. Chem.* **3**, 150-160

31. Kuchar, J., and Hausinger, R. P. (2004) *Chem. Rev.* **104**, 509-526

32. Park, I.-S., Carr, M. B., and Hausinger, R. P. (1994) *Proc. Natl. Acad. Sci. USA* **91**, 3233-3237

33. Park, I.-S., and Hausinger, R. P. (1995) *J. Bacteriol.* **177**, 1947-1951

34. Moncrief, M. B. C., and Hausinger, R. P. (1996) *J. Bacteriol.* **178**, 5417-5421

35. Suh, M. H., Pulakat, L., and Gavini, N. (2003) *J. Biol. Chem.* **278**, 5353-5360

36. Olson, J. W., Fu, C., and Maier, R. J. (1997) *Molec. Microbiol.* **24**, 119-128

37. Olson, J. W., and Maier, R. J. (2000) *J. Bacteriol.* **182**, 1702-1705

38. Rain, J.-C., Selig, L., de Reuse, H., Battaglia, V., Reverdy, C., Simon, S., Lenzen, G., Petel, F., Wojcik, J., Schächter, V., Chemama, Y., Labigne, A., and Legrain, P. (2001) *Nature* **409**, 211--215

39. Heimer, S. R., and Mobley, H. L. (2001) *J. Bacteriol.* **183**, 1423-1433

40. Chang, Z., Kuchar, J., and Hausinger, R. P. (2004) *J. Biol. Chem.* **279**, 15305-15313

41. Mulrooney, S. B., Pankratz, H. S., and Hausinger, R. P. (1989) *J. Gen. Microbiol.* **135**, 1769-1776

CHAPTER 5

Related Studies and Prospects for Future Research

Interactions between UreEF fusion protein and UreG. The UreEF fusion protein interacts with the purified UreD-urease apoprotein complex *in vitro*, and copurifies with other urease components forming a UreD(EF)G-urease apoprotein complex *in vivo* (Chapter 4). To establish possible interactions between UreEF and UreG, Ni-NTA pull-down assays were performed, essentially following the procedures described in Chapter 4. Although there were no stable interactions between these two proteins as evidenced by the lack of the UreG protein in the Coomassie Blue-stained gels, it was still postulated that weak or transient interactions may exist between these molecular chaperone components since they were found in the UreD(EF)G-apoprotein complex. To explore these possibilities, the interactions of the proteins were further examined by western blot analyses after the pull-down assays. As illustrated in Figure 1A, incubation of Ni-NTA resin with purified UreG alone did not result in any significant non-specific binding of the UreG to the resin while the incubation with UreEF-containing cell extracts followed by the purified UreG yielded a UreG immunoreactive band, indicating that the UreEF can specifically interact with UreG in a weak or transient manner. To verify these results, reciprocal pull-down assays were carried out exploiting a biotinylated UreG (encoded by pASK-IBA3G, unpublished data by Soledad Quiroz) and *Strep*-Tactin agarose (IBA, St. Louise). Similarly, the protein-protein interactions were monitored by anti-UreE western blot anayses after *Strep*-Tactin pull-down assays to examine the presence of UreEF in the pooled proteins. The UreEF-containing cell extracts

Figure 1. *In vitro* interactions of UreEF with UreG. **A.** Cell extracts of *E. coli* C41 (DE3)[pET-EF] were incubated with Ni-NTA resin for 15 min at room temperature, and the UreEF-bound resin was incubated with purified UreG for 20 min at room temperature. Eluted proteins were electroblotted to PVDF membranes after SDS-PAGE and probed with anti-UreG antibody. Lanes: M, molecular weight markers; Std, partially purified UreG; G, eluted proteins after incubation of Ni-NTA resin with purified UreG alone; G+EF, eluted proteins after incubation of UreEF-bound Ni-NTA resin with purified UreG. **B.** Cell extracts of *E. coli* DH5α [pASK-IBA3G] were incubated with *Strep*-Tactin resin, and the UreG-bound resin was incubated with the cell extracts of *E. coli* C41 (DE3)[pET-EF] under the same conditions as described for Ni-NTA pull-down assay above. Eluted proteins were subjected to anti-UreE western blot analyses. Lanes: M, molecular weight markers; Std, purified UreEF; EF, eluted proteins after incubation of *Strep*-Tactin resin with the cell extracts of *E. coli* C41 (DE3)[pET-EF]; G+EF, eluted proteins after incubation of UreG-bound *Strep*-Tactin resin with the cell extracts of *E. coli* C41 (DE3)[pET-EF].

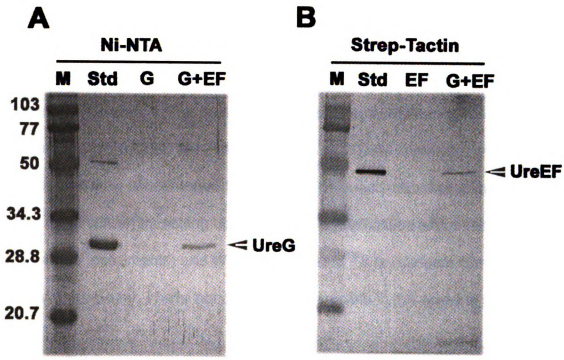
A
Ni-NTA
M
Std
G
G+EF
103
77
50
34.3
28.8
20.7
UreG
B
Strep-Tactin
M
Std
EF
G+EF
UreEF

were used as a negative control to determine if there is any non-specific binding of the UreEF to the resin. As shown in Figure 1B, the UreEF protein was detected only when the biotinylated UreG-bound resin was incubated with the UreEF-containing cell extracts, confirming that there are weak but specific interactions between these two molecular chaperone components *in vitro*.

Crystallization of UreEF. The UreEF fusion protein was purified as described in Chapter 4. The protein was dialyzed against 20 mM Tris buffer (pH 7.8) containing 1 mM EDTA, 2 mM dithiothreitol, 20 mM imidazole, and 10 % glycerol, and then concentrated to 7 mg/ml. The concentrated protein was used for the initial screen by setting up sitting drop crystallization with a robot (IMPAX I-5, Douglas Instruments) and Wizard^{TM}I / Wizard^{TM}II crystallants (Emerald BioSystems). So far, I have not obtained any crystals in the screens yet.

Urease apoprotein activation: refined scheme. Assembly of the urease metallocenter is a complicated process involving nickel, carbon dioxide (used for carbamylation of the bridging lysine residue), several accessory proteins, and GTP hydrolysis. Based on the previous studies by former lab members, a model for *in vivo* urease activation was proposed, as depicted in Figure 2. Sequential binding of UreD, UreF, and UreG to urease apoprotein complex is proposed to enable the formation of productive conformations of the apoprotein complex to accept nickel ions properly. In particular, UreD, UreF, and UreG in combination

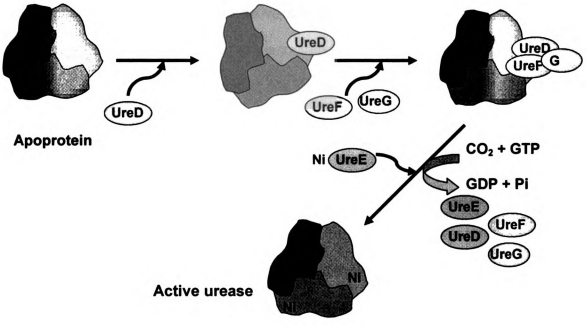

Figure 2. Current model for *in vivo* urease activation. The metallocenter assembly of urease in bacteria is proposed to be a multi-step process typically involving four accessory proteins (UreD, UreE, UreF, and UreG). Urease apoprotein sequentially binds the accessory proteins; first generating the UreD-urease apoprotein complex, followed by binding of UreF, and finally UreG. UreD, UreF, and UreG in combination are proposed to form a GTP-dependent molecular chaperone ensuring productive conformations of the apoproteins for proper metal incorporation while UreE functions as a metallochaperone that binds and delivers Ni to the apoprotein complex. Upon activation, all accessory proteins dissociate from the complex.

are proposed to form a GTP-dependent molecular chaperone (6), which is anticipated to require a functional coordination with UreE serving as a metallochaperone that binds and delivers Ni to the apoprotein complex (1, 5). All accessory proteins are expected to dissociate from the complex after correct incorporation of nickel into the active site as evidenced by the structure of holoenzyme.

In an attempt to characterize UreF as a component of molecular chaperone in the process of urease activation, I generated a soluble form of this molecule as a fusion protein with UreE. The UreEF truncation mutant studies (described in Chapter 4) provided the first evidence for distinct roles of N- and C-termini of the UreF protein in urease activation, presenting more detailed insight into how UreF acts in the process of urease metallocenter assembly. On the basis of my truncation mutant studies and other previous investigations, I propose a model for UreF action in urease activation (Figure 3). The UreF is postulated to act in a two-step process involving the C- and N-termini in a sequential manner. First, the C-terminus of UreF recognizes and binds to the UreD-urease apoprotein complex, primarily interacting with UreD in the apoprotein complex, as supported by previously established interactions between UreD and UreF by yeast-two hybrid (2, 4) and native gel / western blot analyses (3). Then, this initial complex undergoes a conformational change that repositions the N-terminus of UreF so it can interact with other urease component(s). Perhaps these secondary interactions involving the N-terminus may result in a more compact structure of the apoprotein complex such that

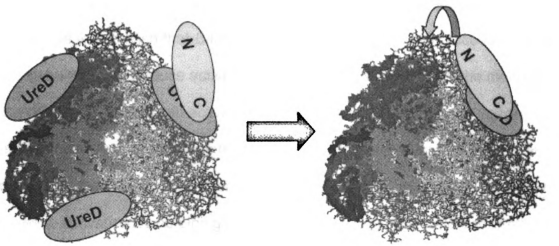

Figure 3. Proposed model for UreF action in urease metallocenter assembly. UreD-urease apoprotein complex is recognized by the C-terminus of UreF. These initial interactions are proposed to induce conformational changes in the complex that position the N-terminus of UreF in an orientation that interacts with other urease component(s) to achieve urease activation.

premature incorporation of nickel into the active site is prevented while UreG can be properly associated with the complex for productive nickel insertion.

Remaining questions and future research. My doctoral research is focused on two different questions on urease activation in bacteria. The first project was to establish that *Bacillus subtilis* (lacking the known accessory genes in its genome) can produce active urease, and then to investigate the mechanism by which this organism can activate urease despite this dearth of accessory genes. The second project was to characterize *Klebsiella aerogenes* UreF, an insoluble urease accessory protein, as an effort to better understand the process of urease activation by obtaining a soluble form of the protein and performing biochemical analyses of the soluble protein. Although my studies on UreF made some contribution to understanding of UreF action in urease activation, many questions still remain to be addressed to elucidate the precise mechanisms of urease activation. As briefly mentioned earlier, the functions of two chaperones (UreDFG molecular chaperone and UreE metallochaperone) are expected to be tightly coordinated for efficient nickel incorporation to the active site. It is unknown how these two chaperones interact with each other in the apoprotein complex, and more importantly, how GTP hydrolysis is coupled to nickel insertion. Of relevance to my studies on UreF, it is unclear whether UreF has additional functions other than inducing conformational changes in the complex by various interactions with other urease components. Furthermore, the consequences of these conformational changes in the complex are not

completely understood yet. As a starting point to answer these questions, crystal structural studies of UreF may provide additional information that is not obtainable by primary sequence analysis, and accordingly, may lead to different perspectives to examine the functions of UreF. Another unknown mechanism concerning the urease activation is how CO_2 enters the active site that is buried in the enzyme and how the active site lysine residue is carbamylated. It needs to be determined whether the carbamylation is a spontaneous process or if some proteins facilitate this process. In particular, it would be intriguing to examine whether UreD or UreF (poorly characterized accessory proteins due to their insolubility) is capable of CO_2 binding so that it can supply CO_2 to the active site more efficiently.

Although the actions of accessory proteins appear to constitute major mechanisms of urease activation in most bacteria, there is an exception to this theme as demonstrated by the case of *B. subtilis* urease. The *B. subtilis* can produce trace levels of urease activity which is sufficient to carry out physiological functions. The mechanism by which this organism generates active nickel-containing urease in the absence of any known accessory proteins is still unclear and needs further investigations.

References

1. Colpas, G. J., and R. P. Hausinger. 2000. In vivo and in vitro kinetics of metal transfer by the *Klebsiella aerogenes* urease nickel metallochaperone, UreE. J. Biol. Chem. 275:10731-10737.

2. Heimer, S. R., and H. L. Mobley. 2001. Interaction of *Proteus mirabilis* urease apoprotein and accessory proteins identified with yeast two-hybrid technology. J. Bacteriol. 183:1423-1433.

3. Moncrief, M. B. C., and R. P. Hausinger. 1996. Purification and activation properties of UreD-UreF-urease apoprotein complexes. J. Bacteriol. 178:5417-5421.

4. Rain, J.-C., L. Selig, H. de Reuse, V. Battaglia, C. Reverdy, S. Simon, G. Lenzen, F. Petel, J. Wojcik, V. Schöhter, Y. Chemama, A. Labigne, and P. Legrain. 2001. The protein-protein interaction map of *Helicobacter pylori.* Nature 409:211-215.

5. Soriano, A., G. J. Colpas, and R. P. Hausinger. 2000. UreE stimulation of GTP-dependent urease activation in the UreD-UreF-UreG-urease apoprotein complex. Biochemistry 39:12435-12440.

6. Soriano, A., and R. P. Hausinger. 1999. GTP-dependent activation of urease apoprotein in complex with the UreD, UreF, and UreG accessory proteins. Proc. Natl. Acad. Sci. 96:11140-11144.